Propofol induces a metabolic switch to glycolysis and cell death in a mitochondrial electron transport chain-dependent manner

Chisato Sumi[1,2], Akihisa Okamoto[2], Hiromasa Tanaka[2], Kenichiro Nishi[2], Munenori Kusunoki[1,2], Tomohiro Shoji[1,2], Takeo Uba[1,2], Yoshiyuki Matsuo[2], Takehiko Adachi[3], Jun-Ichi Hayashi[4], Keizo Takenaga[5] and Kiichi Hirota[2]

[1] Department of Anesthesiology, Kansai Medical University, Hirakata, Japan, [2] Department of Human Stress Response Science, Institute of Biomedical Science, Kansai Medical University, Hirakata, Japan, [3] Department of Anesthesiology, Tazuke Kofukai Medical Institute Kitano Hospital, Osaka, Japan, [4] University of Tsukuba, Tsukuba, Japan, [5] Department of Life Science, Shimane University Faculty of Medicine, Izumo, Japan

Correspondence:
Kiichi Hirota, MD, PhD
Department of Human Stress Response Science
Institute of Biomedical Science
Kansai Medical University
2-5-1 Shin-Machi, Hirakata, Osaka 573-1010, Japan
Tel: +81-72-804-2682
e-mail: hif1@mac.com

Abstract

The intravenous anesthetic propofol (2,6-diisopropylphenol) has been used for the induction and maintenance of anesthesia in operating rooms and for sedation in intensive care units. Although there is no widely accepted definition of propofol infusion syndrome (PRIS), PRIS is defined as the development of metabolic acidosis, rhabdomyolysis, hyperkalemia, hepatomegaly, renal failure, arrhythmia, and progressive cardiac failure. In vitro evidence suggests that PRIS is related to the impaired mitochondrial function. There are indications that preexisting mitochondrial disorders predispose to PRIS. However, the precise molecular mechanisms, including mitochondrial defects and a metabolic conversion by propofol, are largely unknown as yet. To elucidate the underlying cellular and molecular mechanisms of PRIS, we investigated the effects of propofol on the cellular metabolic mode and cell death. We demonstrated that clinically relevant concentrations of propofol, used within a clinically relevant exposure time, suppressed the mitochondrial function, caused the generation of reactive oxygen species, and induced a metabolic switch, from oxidative phosphorylation to glycolysis, by targeting complexes I and III of mitochondria. The data also indicated that a predisposition to mitochondrial dysfunction, caused by a genetic mutation or pharmacological suppression of the electron transport chain by biguanides such as metformin and phenformin, promoted the cell death and caspase activation induced by propofol.

45 **Introduction**

46 Since its introduction into clinical practice in 1986, propofol (2,6-diisopropylphenol)
47 has been used for the induction and maintenance of anesthesia in operating rooms and
48 for sedation in intensive care units [1]. Although propofol is considered a safe agent for
49 anesthesia and sedation, a rare but severe complication can occur, especially in patients
50 receiving high doses of the anesthetic for prolonged periods. A number of clinical
51 reports have indicated a serious side effect of propofol, propofol infusion syndrome
52 (PRIS) [2]. Since PRIS was first described in 1992 [3], the clinical awareness and research
53 interest into this disorder have continued to grow. The medical literature now includes
54 over 100 published case reports, case series, and reviews. Nonetheless, the exact
55 incidence and etiology of PRIS remain unclear at present. Although there is no widely
56 accepted definition of PRIS, PRIS is defined as the development of metabolic acidosis
57 (lactic acidosis), rhabdomyolysis, hyperkalemia, hepatomegaly, renal failure,
58 arrhythmia, and progressive cardiac failure [2]. There is a strong association between
59 PRIS and propofol infusion at doses greater than 4 mg/kg/h and an exposure longer than
60 48 h, although the precise molecular mechanisms of PRIS have not been elucidated. In
61 vitro evidence suggests that PRIS is related to impaired mitochondrial function [4]. There
62 are indications that preexisting mitochondrial disorders predispose to PRIS [4-6].
63 Moreover, studies using isolated mitochondria have demonstrated that propofol showed
64 an effect on the mitochondrial respiratory chain. A decrease in the transmembrane
65 electrical potential ($\Delta\Psi$) has been reported in liver mitochondria isolated from rats
66 incubated with propofol [7]. An increase of the oxygen consumption rate (OCR) has
67 suggested that propofol acts as an uncoupler in oxidative phosphorylation (OXPHOS) [8].
68 It has also been indicated that incubation of isolated mitochondria from rats with high

69 concentrations of propofol (100 to 400 μM) resulted in a strong inhibition of the activity
70 of complex I and, to a lesser degree, of complexes II and III [9]. Other reports have also
71 demonstrated a reduction of complex IV activity in skeletal muscles, which led to a
72 hypothesis that a propofol metabolite causes a disruption of the respiratory chain [10].
73 However, the precise molecular mechanisms, including the relationship between
74 mitochondrial defects and metabolic reprogramming in the pathophysiology of PRIS,
75 are largely unknown as yet. To investigate the underlying cellular and molecular
76 mechanisms of PRIS, we investigated the effects of propofol on cell life and death,
77 oxygen metabolism, and mitochondrial function using cells of various origins, including
78 transmitochondrial cybrid cells harboring a mitochondrial DNA defect and mutations.
79 We demonstrated that clinically relevant concentrations of propofol, used within a
80 clinically relevant exposure time, suppressed the mitochondrial function, caused the
81 generation of reactive oxygen species (ROS), and induced the metabolic reprogramming
82 [11], from OXPHOS to glycolysis, by targeting complexes I and III of mitochondria. The
83 data also indicated that a predisposition to mitochondrial dysfunction, caused by a
84 genetic mutation or pharmacological suppression of the electron transport chain (ETC)
85 in mitochondria by biguanides such as metformin and phenformin, promoted the cell
86 death and caspase activation induced by propofol.
87

Results

Propofol induced cell death and activation of caspases in a concentration- and time-dependent manner

To determine whether propofol induces the cell death, we examined the concentration- and time-response relationship between propofol and cell death. Neuronal SH-SY5Y cells were treated with the indicated concentrations of propofol and for the indicated times. Cells were stained with propidium iodide (PI) and recombinant fluorescein isothiocyanate (FITC)-conjugated annexin V, and the proportion of dead cells was evaluated by flow cytometry. Concentrations of propofol equal to or greater than 50 μM induced the cell death within 6 h (Figs. 1a and 1b). Interestingly, 25 μM propofol induced the cell death at a longer incubation, 12 h (Fig. 1c). Next, activities of caspase-9 and caspase-3/7 were evaluated. Propofol at concentrations equal to or greater than 50 μM activated caspase-9 (Fig. 2a). As in the case of cell death and caspase-9, caspase-3/7 was activated by the treatment with 50 μM or greater propofol concentrations within 6 h. Importantly, 25 μM propofol, which did not induce caspase-3/7 activation within 6 h (Fig. 2b), induced the activation at 12 h (Fig. 2c). Next, a release of lactate dehydrogenase (LDH) was investigated (Fig. 2d). Within 6 h, only propofol at a concentration of 150 μM increased the LDH release. On the other hand, during 12-h incubation, not only 150 μM but also 50 and 100 μM propofol statistically significantly increased the LDH release. Measurement of the mitochondrial membrane voltage ($\Delta\Psi m$) showed that propofol at concentrations equal to or greater than 50 μM decreased $\Delta\Psi m$ within 6 h (Fig. 2e). In addition, at concentrations higher than 50 μM propofol suppressed the cell viability, measured by an MTS [3-(4,5-dimethylthiazol-2-yl)-5-(3-carboxymethoxyphenyl)-2-(4-sulfophenyl)-2*H*-tetrazolium] assay, within 6 h

112 (Supplementary Fig. 1a). 2,4-Diisopropylphenol, commonly known as 2,4-propofol, is
113 an isomeric form of propofol, which does not show a hypnotic effect. We tested the
114 effects of 2,4-diisopropylphenol on caspase-3/7 activation in SH-SY5Y cells. Similar to
115 propofol, 2,4-diisopropylphenol induced caspase-3/7 activation within 6 h
116 (Supplementary Fig. 1b). Interestingly, 25 μM 2,4-diisopropylphenol could activate
117 caspase-3/7 within 6 h, suggesting that 2,4-diisopropylphenol is more toxic than
118 propofol. Finally, the effects of propofol were investigated in cells of different origins,
119 including mouse myoblast C2C12 cells (Supplementary Fig. 1c), human cervical cancer
120 HeLa cells (Supplementary Fig. 1d), and Lewis lung carcinoma P29 cells
121 (Supplementary Fig. 1e). Similar to its effects on SH-SY5Y cells, 50 and 100 μM
122 propofol but not 12.5 or 25 μM propofol induced caspase-3/7 activation in the other cell
123 lines within 6 h.
124
125 **Propofol suppressed oxygen metabolism and induced ROS generation**
126 We investigated the effects of propofol on oxygen metabolism and glycolysis in SH-
127 SY5Y cells by assaying OCR and the extracellular acidification rate (ECAR), which is a
128 surrogate index for glycolysis. SH-SY5Y cells were preincubated with the indicated
129 concentrations of propofol for the indicated periods. The mitochondrial OCR was
130 significantly suppressed by the treatment with 50 μM propofol for 6 h (Figs. 3a and 3b,
131 Supplementary Figs. 2a and 2c–f). Accordingly, the ECAR levels were significantly
132 higher upon the treatment with 50 μM propofol (Figs. 3c and 3d, Supplementary Fig.
133 2b). Propofol at a concentration of 25 μM, which exerted no significant effects within 6
134 h, suppressed OCR (Fig. 3e) and enhanced ECAR (Fig. 3f) after 12 h of incubation.
135 Thus, the evidence indicates that propofol affects the oxygen metabolism in

136 mitochondria. It has been reported that the disturbance of the mitochondrial ETC leads
137 to the generation of ROS by cells [12,13]. ROS generation was observed in SH-S5Y5 cells
138 in response to propofol exposure within 3 and 6 h (Fig. 3g). Cell death was suppressed
139 by the treatment with 10 mM *N*-acetylcysteine (Fig. 3h).
140
141 **Involvement of mitochondria in propofol-induced cell death and caspase activation**
142 As shown in figure 3, propofol affected the mitochondrial ETC and intracellular oxygen
143 metabolism in SH-SY5Y cells. To examine the involvement of mitochondria in
144 propofol-induced cell death, we used the P29 cell line and its derivative ρ0P29, which
145 lacks the mitochondrial DNA (mtDNA) [14-16]. P29 and ρ0P29 cells were exposed to the
146 indicated concentrations of propofol for 6 h, and then cell death (Fig. 4a) and the
147 activity of caspase-3/7 (Fig. 4b) were assayed. Both cell death and caspase-3/7 assays
148 indicated that, unlike P29 cells, ρ0P29 cells were completely resistant to 50 μM and
149 partially resistant to 100 μM propofol after 6 h of incubation (Figs. 4a and 4b). Together
150 with the results showing that propofol affects the ETC function of mitochondria, this
151 evidence strongly suggests that mitochondria play a critical role and are one of the
152 targets in propofol-induced cell death.
153
154 **Effects of propofol on the ETC complex-dependent OCR**
155 Next, we examined the oxygen consumption, which depends on the activity of
156 mitochondrial respiratory chain complexes I–IV in membrane-permeabilized and intact
157 cells, using an Extracellular Flux Analyzer™ (Supplementary Fig. 3). OCR traces of
158 mitochondrial respiration were detected using protocol A (Fig. 5a, Supplementary Fig.
159 3a) and protocol B (Fig. 5b, Supplementary Fig. 3b). The results indicated that propofol

160 significantly suppressed the complex I- and complex III-dependent OCR but not the
161 complex II- or complex IV-dependent OCR (Figs. 5c–5d).
162
163 **Mitochondrial ETC inhibitors synergistically enhanced propofol toxicity**
164 We investigated the effects of several ETC inhibitors on the propofol-induced cell death
165 in SH-SY5Y cells. Cells were exposed to rotenone (100 nM), antimycin A (25 μg/mL),
166 or oligomycin (4 μM), with or without the indicated concentrations of propofol, for 6 h,
167 and cell death was assayed by flow cytometry. Neither 100 nM rotenone, 25 μg/mL
168 antimycin, 4 μM oligomycin, nor 12.5 μM or 25 μM propofol alone induced the cell
169 death within 6 h (Fig. 6a). On the other hand, 12.5 and 25 μM propofol induced the cell
170 death in the presence of rotenone, antimycin A, and oligomycin (Fig. 6a). Similarly,
171 12.5 and 25 μM propofol with rotenone, antimycin A, and oligomycin induced the
172 caspase-3/7 activity within 6 h (Fig. 6b). The evidence indicates that cooperative
173 inhibition of mitochondria by both propofol and the ETC inhibitors induces cell death at
174 even clinically relevant concentrations of propofol within 6 h.
175
176 **Genetic predisposition to mitochondrial dysfunction increased propofol-induced**
177 **caspase activation and cell death**
178 For further study, we used transmitochondrial cybrids carrying mtDNA with defined
179 pathogenic mutations. mtDNA donors and ρ0P29 cells were used to obtain
180 transmitochondrial cybrids P29mtA11, P29mtB82M, P29mtCOIM, and P29mtΔ
181 (Tables 2 and 3) [16], and oxygen metabolism profiles of these clones were examined
182 (Figs. 7a and 7b). These transmitochondrial cybrids were exposed to the indicated
183 concentrations of propofol for 6 h to investigate the cell death and caspase-3/7

184 activation. Interestingly, in contrast to parental P29 cells, the cell death flow cytometry
185 assay indicated that 25 μM propofol induced the cell death within 6 h in P29mtA11,
186 P29mtB82M, and P29mtCOIM cells (Fig. 7c). Caspase-3/7 activation was also induced
187 in P29mtA11, P29mtB82M, and P29mtCOIM cells even with 25 μM propofol (Fig. 7d).
188 In contrast, P29mtΔ cells, similar to ρ0P29 cells, were completely resistant to 50 μM
189 propofol and partially resistant to 100 μM propofol (Fig. 7d). Thus, our experimental
190 results indicated that cells harboring genetic mutations in mtDNA (*ND6* in complex I or
191 *COI* in complex IV) were more susceptible to propofol.
192 ROS generation was investigated in P29 cells, P29mtA11 cells and ρ0P29 cells in
193 response to propofol exposure. Cells were exposed to 25 μM propofol for 6 h.
194 P29mtA11 cells produced more ROS compared to P29 cells. 25 μM propofol, which did
195 not produce ROS in P29 cells, induced generation of more ROS in P29mtA11 cells. In
196 contrast, ρ0P29 cells did not produce ROS even under 50 μM propofol.
197 Accordingly, cell death induced by 25 μM propofol was suppressed by treatment with
198 10 mM NAC.
199
200 **Pharmacological suppression of mitochondrial ETC increased propofol-induced**
201 **cell death and caspase activation**
202 The biguanides metformin and phenformin are widely used to reduce high blood sugar
203 levels caused by diabetes [17]. Metformin and phenformin have also been shown to
204 suppress complex I of ETC, which is used by cells to generate energy [18-22]. To confirm
205 the effect of blockade of ETC, SH-SY5Y cells were pretreated with 2.5–20 mM
206 metformin or 5–15 μM phenformin for 6 h, with or without the indicated concentrations
207 of propofol, and then the cells were tested using the OCR and ECAR assays. Incubation

208 for 6 h with either 2.5 mM metformin or 5 μM phenformin did not affect OCR (Fig. 8a
209 and Supplementary Fig. 4a) and ECAR (Fig. 8b and Supplementary Fig. 4b) in SH-
210 SY5Y cells. In contrast, not only 25 μM but also 12.5 μM propofol, which did not affect
211 OCR or ECAR alone, significantly decreased OCR (Fig. 8a) and increased ECAR (Fig.
212 8b) in the presence of 2.5 mM metformin. Next, we investigated ROS generation upon
213 cell exposure to 25 μM propofol with or without 5 mM metformin. Exposure to 25 μM
214 propofol did not induce ROS generation without metformin. With metformin, however,
215 25 μM propofol induced ROS generation (Fig. 8c). Then, SH-SY5Y cells were tested
216 for cell death (Fig. 8d) and caspase 3/7 activation (Fig. 8e) after treatment with 5 mM
217 metformin or 5 μM phenformin (Supplementary Figs. 4c and 4d) for 6 h, with or
218 without the indicated concentrations of propofol. Metformin at 5 mM and phenformin at
219 5 μM increased the propofol-induced cell death and caspase-3/7 activation.

220 **Discussion**

221 In this study, we demonstrated for the first time that propofol at clinically relevant
222 concentrations and within clinically relevant incubation times altered the oxygen
223 metabolism by targeting mitochondrial complexes I and III and induced a cellular
224 metabolic switch, from OXPHOS to glycolysis, and generation of ROS. The
225 suppression of mitochondria elicited the cell death in cell lines of various origins,
226 including transmitochondrial cybrids carrying mtDNA with defined pathogenic
227 mutations.

228 The concentrations of propofol tested in this study varied from 12.5 to 150 μM. It has
229 been reported that the plasma concentrations of propofol during anesthesia and sedation
230 are from 2 μg/mL (11 μM) up to 5 μg/mL (27.5 μM) [23]. The concentration of propofol
231 was also measured in tissue samples from rats treated with propofol at a dose of 20
232 mg/kg/h, and the study indicated that the tissue concentration of propofol could reach
233 200 μM under certain conditions [24]. Thus, the evidence indicates that the concentrations
234 of propofol used in this study were clinically relevant. The duration of exposure used in
235 this study ranged from 3 to 12 h, which was also within the clinically relevant period of
236 exposure.

237 Although predictive factors for PRIS have not been established, there is a consensus
238 that exposure to high doses of propofol for prolonged periods is the most critical risk
239 factor for PRIS [1,2,6,25]. In this study, we demonstrated that propofol at concentrations
240 equal to or greater than 50 μM but not at or below 25 μM showed cell toxicity within 6
241 h. On the other hand, even 25 μM propofol significantly increased the cell death and
242 caspase activity during incubation for 12 h (Figs. 1b and 1f). In addition, propofol at 50
243 and 25 μM significantly suppressed OCR and increased ECAR within 6 and 12 h,

244 respectively. At 100 μM, propofol inhibited both OCR and ECAR, which could be due
245 to a rapid cell death induced by 100 μM propofol. The evidence indicates that propofol
246 at clinically relevant concentrations suppresses OXPHOS and induces a metabolic
247 switch, from OXPHOS to glycolysis, resulting in the enhancement of lactate
248 production. This metabolic conversion can be one of the most critical cellular
249 mechanisms of lactic acidosis observed in PRIS [1,2].
250 As clearly demonstrated in this and other studies [26-29], propofol induces cell death. In
251 this study, we demonstrated that not only neuronal SH-SY5Y cells but also cells of
252 other origins, such as C2C12 muscle cells, HeLa cervical carcinoma cells, and P29 lung
253 cancer cells, are susceptible to propofol. Although there is no consensus on the target
254 organs or tissues in the context of PRIS, our results suggest that propofol can exert
255 toxicity against a wide range of tissues.
256 There are at least two known modes of cell death, apoptosis and necrosis. Apoptosis is a
257 strictly regulated or programmed process involving the activation of specific proteases,
258 which are responsible for organized removal of damaged cells [30]. Necrosis is a
259 pathophysiologically different form of cell death, which is accompanied by a loss of
260 $\Delta\psi m$ and impairment of OXPHOS. In this study, propofol treatment promoted the
261 caspase-9 and caspase-3/7 activation. These data indicate that propofol at least activates
262 the apoptosis pathway. Meanwhile, the flow cytometry analysis demonstrated that
263 treatment of cells with propofol concentrations greater than 50 μM for 12 h also resulted
264 in an LDH release (Fig. 1d) and increased the PI^+/annexin V^- cell population, in
265 addition to the PI^+/annexin V^+ cell population (Fig. 1a). These data strongly suggest that
266 propofol elicits both types of cell death, resulting in cell membrane injury at a 50 μM
267 concentration and 12-h exposure.

268 As demonstrated in figures 2 and 3, propofol inhibited the mitochondrial oxygen
269 consumption in a time- and concentration-dependent manner. In this study, we measured
270 OCR, which is dependent on the activity of each ETC complex in intact cells, using an
271 extracellular flux analyzer. Several studies have used isolated mitochondria, and some
272 have suggested that propofol inhibits the enzymatic activity of complexes II and IV [31].
273 However, our study using intact cells indicated that propofol does not affect the
274 complex II- or complex IV-dependent OCR. Another finding was that propofol induced
275 ROS generation (Fig. 2g). While the precise origin of ROS remains unclear, our
276 findings strongly suggest that mitochondria play a critical role in this process. ρ0P29
277 cells and P29mtΔ cells did not produce ROS in response to propofol treatment (data not
278 shown). It has been demonstrated that the disturbance of mitochondria leads to
279 increased production of ROS by ETC [12,13,32-34]. In fact, cybrid cells such as P29mtA11
280 and P29mtB82M with a mutation in the mitochondrial NADH dehydrogenase subunit 6
281 (*ND6*) gene generate ROS under 20% O_2 conditions [16,35], which implies that propofol-
282 mediated cell death is dependent on ROS from mitochondria. Mitochondrial disease,
283 once thought to be a rare clinical entity, is now recognized as an important cause of a
284 wide range of neurological, cardiac, muscle, and endocrine disorders [4,5]. It has been
285 reported that complex I is uniquely sensitive to many anesthetic agents [36]. To approach
286 the issue, we used cells harboring mtDNA mutations [15,16,37]. As shown in figures 3 and
287 6, ρ0P29 cells, which do not have mtDNA, are resistant to 50 μM propofol. P29mtΔ
288 cells, carrying the nuclear genome of P29 cells and the mitochondrial genome of
289 ΔmtDNA4696, with a 4,696-bp deletion [15], are also resistant to propofol. In contrast,
290 P29mtA11 cells with the G13997A mutation in mtDNA and P29mtB82M cells with the
291 13885insC insertion, both of which affect the NADH-ubiquinone oxidoreductase chain

292 6 (ND6) protein of complex I, are more sensitive to propofol than P29 cells are.
293 Propofol at 12.5 and 25 μM induced the cell death and caspase-3/7 activation in both
294 mutant cell lines within 6 h (Fig. 6c). This is consistent with the evidence showing that
295 25 μM propofol induced the cell death in the presence of a sublethal concentration of
296 rotenone. P29mtCOIM cells with a missense mutation in cytochrome c oxidase I (COI)
297 are as sensitive to propofol as P29mtA11 and P29mtB82M cells. This is also consistent
298 with the result showing that propofol induced the cell death in the presence of
299 oligomycin (Fig. 5). This evidence indicates that cells with mutations in mtDNA are
300 more sensitive to propofol.
301 In addition to the genetic mutations affecting mitochondrial function, pharmacological
302 disturbance of mitochondria with biguanides, including metformin and phenformin, also
303 synergistically suppressed the mitochondrial function and induced caspase activation
304 and cell death. The primary effect of biguanides is generally thought to be the inhibition
305 of respiratory complex I (NADH:ubiquinone oxidoreductase), which leads to the energy
306 stress by decreasing ATP synthesis by OXPHOS [18,19,38,39]. In addition, a number of
307 studies have indicated that biguanides also affect complexes II, III, and IV and F1F0-
308 ATPase [20,40]. Metformin and phenformin are used as antidiabetic drugs and are
309 associated with lactic acidosis [20,41,42]. As demonstrated in this study, both metformin and
310 phenformin increased ECAR and decreased OCR, which indicates a metabolic switch.
311 In addition to biguanides, other clinically used drugs, including chloramphenicol [43,44],
312 aspirin [45,46], statins [18], and local anesthetics [47], also inhibit mitochondrial functions. Our
313 results indicate that pre-exposure to mitochondrial inhibitors may increase the toxicity
314 of propofol.

315 There are some limitations in this study. Thus, we only used cultured cells. Because
316 PRIS is a systemic syndrome, using cells is not sufficient to completely understand the
317 pathophysiology of PRIS. An *in vivo* investigation using experimental animals may be
318 warranted to confirm our findings.
319 In conclusion, clinically relevant concentrations of propofol used within a clinically
320 relevant exposure time suppressed the mitochondrial function, caused the generation of
321 ROS, and induced metabolic reprogramming, from OXPHOS to glycolysis, by targeting
322 complexes I and III of mitochondria. Our data also indicated that a predisposition to
323 mitochondrial dysfunction, caused by genetic mutations and pharmacological
324 suppression of ETC by biguanides such as metformin and phenformin, promoted the
325 cell death and caspase activation by propofol. The process is likely to constitute the
326 molecular basis of PRIS.
327

Materials and Methods

Reagents

Propofol (2,6-diisopropylphenol), 2,4-diisopropylphenol, and dimethyl sulfoxide were obtained from Sigma–Aldrich (St. Louis, MO, USA). Rotenone, oligomycin, and antimycin A were obtained from Abcam, Inc. (Cambridge, MA, USA). The Key Resources Table is provided as Table 1.

Cell lines and cell culture

Established cell lines derived from human neuroblastoma SH-SY5Y cells and cervical carcinoma HeLa cells were maintained in RPMI 1640 medium supplemented with 10% fetal bovine serum, 100 U/mL penicillin, and 0.1 mg/mL streptomycin. The mouse cell lines and their characteristics are listed in Tables 2 and 3. P29 cells originated from Lewis lung carcinoma (C57BL/6 mouse strain), and B82 cells are fibrosarcoma cells derived from the L929 fibroblast cell line (C3H/An mouse strain) [15,16,48]. Parental P29 cells, ρ0 cells, and the transmitochondrial cybrids were grown in Dulbecco's modified Eagle's medium (DMEM) supplemented with pyruvate (0.1 mg/mL), uridine (50 mg/mL), and 10% fetal bovine serum. We isolated ρ0 cells by treating parental P29 cells with 1.5 mg/mL ditercalinium, an antitumor *bis*-intercalating agent. Enucleated cells of mtDNA donors were prepared by pretreatment with cytochalasin B (10 μg/mL) for 2 min, followed by centrifugation at 7,500 × *g* for 10 min [16]. The resultant cytoplasts were fused with ρ0 cells using polyethylene glycol. The transmitochondrial cybrids (see Table 3) were isolated in a selection medium that allows exclusive growth of the cybrids [16].

352 **Cell growth MTS assay**

353 Cell growth was assessed using a CellTiter 96 AQueous One Solution Cell Proliferation
354 Assay™ with MTS (Promega, Madison, WI, USA) [47,49]. Briefly, cells were seeded into
355 96-well plates (2×10^4 cells/well) and cultured overnight. On the following day, the
356 cells were treated with the indicated concentrations of the appropriate drug(s) for
357 varying times. After the treatment, 20 μL of the CellTiter 96 AQueous One Solution™
358 reagent was added to each well, the plates were incubated at 37 °C for 1 h, and the
359 absorbance of each sample was measured using an iMark™ microplate reader (Bio-
360 Rad, Hercules, CA, USA) at a wavelength of 490 nm. Cell viability was calculated by
361 comparing the absorbance of treated cells with that of the control cells incubated
362 without drugs, which was defined as 100%. All samples were tested in triplicate or
363 quadruplicate in each experiment.

364

365 **Caspase-3/7 and caspase-9 activity assays**

366 Activity levels of caspase-3/7 and caspase-9 were assessed using an Apo-ONE™
367 homogeneous caspase-3/7 assay kit (Promega) and a Caspase-Glo™ 9 assay kit
368 (Promega), respectively, according to the manufacturer's protocols [47,49]. Briefly, cells
369 were seeded into 96-well plates (2×10^4 cells/well) and incubated overnight. On the
370 following day, the cells were treated with the indicated concentrations of the appropriate
371 drug(s) for varying times. After the treatment, 100 μL of the Apo-ONE™ caspase-3/7
372 reagent was added to each well. The plates were incubated at room temperature for 1 h,
373 and the luminescence of each well was measured using an EnSpire™ multimode plate
374 reader (PerkinElmer, Waltham, MA, USA). Caspase activity was calculated by
375 comparing the levels of luminescence of the treated cells with that of the control cell

376 population incubated without drugs, which was defined as 100%. The assays were
377 performed in triplicate at least twice. Data were expressed as the mean ± standard
378 deviation (SD).
379
380 **Analysis of cell death**
381 The protocol was described previously [47,49]. Briefly, the levels of cell apoptosis were
382 measured using an Annexin V–FITC apoptosis detection kit (BioVision, Milpitas, CA,
383 USA), according to the manufacturer's instructions. For the analysis, cells were seeded
384 into 6-well plates (3×10^5 cells/well) and incubated overnight. On the following day,
385 the cells were treated with the indicated concentrations of the appropriate drug(s) for
386 varying times and harvested by centrifugation at 1,200 rpm for 3 min. The cell pellets
387 were resuspended in a mixture comprised of 500 μL of binding buffer, 5 μL of annexin
388 V–FITC, and 5 μL of PI (50 μg/mL). The suspensions were incubated for 5 min at room
389 temperature in the dark and analyzed using a FACSCalibur flow cytometer (BD
390 Biosciences, San Jose, CA, USA) equipped with the CellQuest Pro™ software. The data
391 were evaluated using the FlowJo™ version 9.9.4 software (TreeStar, Ashland, OR,
392 USA), then exported to Excel spreadsheets, and subsequently analyzed using the
393 statistical application GraphPad™ Prism 7.
394
395 **Determination of mitochondrial membrane potential**
396 The mitochondrial membrane potential (ΔΨm) was determined by flow cytometry using
397 a MitoPT™ JC-1 assay kit (ImmunoChemistry Technologies, Bloomington, MN, USA),
398 according to the manufacturer's instructions [49]. For the analysis, cells were seeded into
399 6-well plates (3×10^5 cells/well) and cultured overnight. On the following day, the cells

400 were treated with the indicated concentrations of the appropriate drug(s) for varying
401 times and then pelleted by centrifugation at 1,200 rpm for 3 min. The cells were then
402 resuspended in JC-1, incubated at 37 °C for 15 min in the dark, and collected by
403 centrifugation at 1,200 rpm for 3 min. The cell pellets were resuspended in 500 μL of
404 assay buffer. The samples were subsequently analyzed using a FACSCalibur flow
405 cytometer (BD Biosciences) equipped with the CellQuest Pro™ software for the
406 detection of red JC-1 aggregates (590 nm emission) or green JC-1 monomers (527 nm
407 emission). The data were evaluated using the FlowJo version 7.6.3 software (TreeStar),
408 then exported to Excel spreadsheets, and subsequently analyzed using the statistical
409 application GraphPad™ Prism 7.
410
411 **LDH-based cytotoxicity assay**
412 Cytotoxicity was measured using a CytoTox-ONE™ kit (Promega) as described
413 previously [47,49]. Briefly, cells were cultured overnight in 96-well plates (2×10^4
414 cells/well) and treated with the indicated drug(s) for varying lengths of time. Twenty
415 microliters of the CytoTox-ONE™ reagent was added to each well, and the plates were
416 incubated at 22 °C for 10 min. The reaction was terminated by adding 50 μL of the stop
417 solution, and the fluorescence was recorded at an excitation wavelength of 560 nm and
418 an emission wavelength of 590 nm using an EnSpire™ multimode plate reader
419 (PerkinElmer). The percentage of cell death was determined by comparing the release
420 of LDH (fluorescence value) in each treatment group with that of the positive control
421 treated with the lysis solution, which was defined as 100%. Meanwhile, the level of
422 LDH release from untreated cells (negative control) was defined as 0%. Each sample
423 was assayed in triplicate.

424

425 **Measurement of ROS generation**

426 ROS generation was detected with 2′,7′-dichlorofluorescin diacetate (DCFH-DA)
427 (Molecular Probes, Eugene, OR, USA). Briefly, cells cultured in 35-mm-diameter glass-
428 bottom culture dishes (MatTek, Ashland, MA, USA) were incubated with 10 μM
429 DCFH-DA for 10 min at 37 °C in a serum-free DMEM, then washed twice with
430 Dulbecco's phosphate-buffered saline, and analyzed using a flow cytometer (Beckton
431 Dickinson). The mean fluorescence intensity was analyzed using the CellQuest software
432 (Becton Dickinson).

433

434 **Cellular oxygen consumption and extracellular acidification measurement**

435 Cellular OCR and ECAR were determined with the XF Cell Mito Stress Test™ and XF
436 Glycolysis Stress Test™, respectively, using an XFp Extracellular Flux Analyzer™
437 (Seahorse Bioscience, USA) [47]. Cells (2×10^5 cells/well) were seeded into an XFp cell
438 culture microplate, and OCR was assessed in glucose-containing XF base medium
439 according to the manufacturer's instructions. The sensor cartridge for the XFp analyzer
440 was hydrated in a 37 °C non-CO_2 incubator on the day before the experiment. For the
441 OCR assay, injection port A on the sensor cartridge was loaded with 1.5 μM oligomycin
442 (complex V inhibitor), port B was loaded with 2 μM carbonyl cyanide-4-
443 (trifluoromethoxy) phenylhydrazone (FCCP), and port C was loaded with 0.5 μM
444 rotenone/antimycin A (inhibitors of complex I and complex III). During the sensor
445 calibration, cells were incubated in a 37 °C non-CO_2 incubator in 180 μL of assay
446 medium (XF base medium with 5.5 mM glucose, 1 mM pyruvate, and 2 mM L-
447 glutamine, pH 7.4). The plate was immediately placed into the calibrated XFp

448 extracellular flux analyzer for the Mito Stress test (Supplementary Fig. 3a). The assay
449 parameters were calculated as follows: OCR (basal) = (last rate measurement before
450 oligomycin injection) − (minimum rate measurement after rotenone/antimycin-A
451 injection); OCR (maximal) = (maximum rate measurement after FCCP injection) −
452 (minimum rate measurement after rotenone/antimycin A injection); OCR (non-
453 mitochondrial respiration) = (minimum rate measurement after rotenone/antimycin A
454 injection); proton leak = (minimum rate measurement after oligomycin injection) –
455 (non-mitochondrial respiration). For the ECAR assay, injection port A on the sensor
456 cartridge was loaded with 10 mM glucose. During the sensor calibration, cells were
457 incubated in a 37 °C non-CO_2 incubator in 180 μL of assay medium (XF base medium
458 with 2 mM L-glutamine, pH 7.4). The plate was immediately placed into the calibrated
459 XFp Extracellular Flux Analyzer™ for the Glycolysis Stress test (Supplementary Fig.
460 3b). Oligomycin (1 μM) and 50 mM 2-deoxy-D-glucose were loaded for the
461 measurement. ECAR was normalized for the total protein/well and calculated as
462 follows: ECAR (glycolysis) = (maximum rate measurement after glucose injection) −
463 (last rate measurement before glucose injection).
464
465 **Measurement of oxygen consumption in permeabilized cells**
466 The activity of individual respiratory chain complexes was evaluated in permeabilized
467 cells [50,51]. Briefly, cells were washed with MAS buffer (220 mM mannitol, 70 mM
468 sucrose, 10 mM KH_2PO_4, 5 mM $MgCl_2$, 2 mM HEPES, 1 mM EGTA, 0.2% fatty acid-
469 free bovine albumin, adjusted to pH 7.2 with KOH), and the medium was replaced with
470 MAS buffer supplemented with 10 mM pyruvate, 1 mM malate, 4 mM ADP, and 1 nM
471 plasma membrane permeabilizer™. The cells were then loaded into the XFp analyzer to

472 measure respiration rates using cycles of 30 s mixing/30 s waiting/2 min measurement.
473 After measurement of pyruvate-driven respiration, rotenone (final concentration: 2 μM)
474 was injected through port A to halt the complex I-mediated respiratory activity. Next,
475 succinate (10 mM) was injected through port B to donate electrons at complex II,
476 bypassing complex I inhibition. Addition of antimycin A (2 μM) via port C inhibited
477 complex III, and N,N,N′,N′-tetramethyl-*p*-phenylenediamine (0.1 mM), combined with
478 ascorbate (10 mM), was subsequently injected through port D to measure complex IV
479 activity. As an alternative approach, cells were initially provided with pyruvate to
480 measure complex I activity. After injection of rotenone, duroquinol was injected to
481 stimulate complex III-mediated respiration.
482
483 **Statistical analysis**
484 All experiments were repeated at least twice, and each sample was evaluated in
485 triplicate. Representative data, expressed as the mean ± SD, are shown. Differences
486 between treatment groups were evaluated by one-way analysis of variance (ANOVA) or
487 two-way ANOVA, followed by Dunnett's multiple comparison test or *t*-test using
488 GraphPad Prism 7. P-values of < 0.05 were considered statistically significant.
489

Acknowledgments

This work was supported by the Japan Society for the Promotion of Science KAKENHI, grants #26670693 and #24592336 to K.H., #25462457 to K.N., and #15K15577 to T.A, a research grant from Katano Kai to K.H. and A.O., research grant B from Kansai Medical University to A.O., and a KMU consortium grant from Kansai Medical University to K.H.

We would like to thank Editage (www.editage.jp) for English language editing.

Author contributions statement

C.S. performed the experiments, analyzed the data, and co-wrote the manuscript. A.O., M.T., M.K., H.S., T.U., Y.M., and T.A. contributed to the data analysis and discussion. J.H. and K.T. provided experimental materials and contributed to the discussion. K.H. designed and supervised the study, analyzed the data, and co-wrote the manuscript.

Additional information

Competing financial interests

The authors declare no competing financial interests.

510 **References**

511 1 Kam, P. C. & Cardone, D. Propofol infusion syndrome. *Anaesthesia* **62**, 690-
512 701, doi:10.1111/j.1365-2044.2007.05055.x (2007).
513 2 Bray, R. J. Propofol infusion syndrome in children. *Paediatr Anaesth* **8**, 491-499
514 (1998).
515 3 Parke, T. J. *et al.* Metabolic acidosis and fatal myocardial failure after propofol
516 infusion in children: five case reports. *BMJ* **305**, 613-616 (1992).
517 4 Finsterer, J. & Frank, M. Propofol Is Mitochondrion-Toxic and May Unmask a
518 Mitochondrial Disorder. *J Child Neurol* **31**, 1489-1494,
519 doi:10.1177/0883073816661458 (2016).
520 5 Niezgoda, J. & Morgan, P. G. Anesthetic considerations in patients with
521 mitochondrial defects. *Paediatr Anaesth* **23**, 785-793, doi:10.1111/pan.12158
522 (2013).
523 6 Fudickar, A. & Bein, B. Propofol infusion syndrome: update of clinical
524 manifestation and pathophysiology. *Minerva Anestesiol* **75**, 339-344 (2009).
525 7 Bains, R., Moe, M. C., Vinje, M. L. & Berg-Johnsen, J. Sevoflurane and
526 propofol depolarize mitochondria in rat and human cerebrocortical
527 synaptosomes by different mechanisms. *Acta Anaesthesiol Scand* **53**, 1354-
528 1360, doi:10.1111/j.1399-6576.2009.02047.x (2009).
529 8 Branca, D., Roberti, M. S., Vincenti, E. & Scutari, G. Uncoupling effect of the
530 general anesthetic 2,6-diisopropylphenol in isolated rat liver mitochondria. *Arch*
531 *Biochem Biophys* **290**, 517-521 (1991).
532 9 Rigoulet, M., Devin, A., Averet, N., Vandais, B. & Guerin, B. Mechanisms of
533 inhibition and uncoupling of respiration in isolated rat liver mitochondria by the

534 general anesthetic 2,6-diisopropylphenol. *Eur J Biochem* **241**, 280-285 (1996).
535 10 Cray, S. H., Robinson, B. H. & Cox, P. N. Lactic acidemia and bradyarrhythmia
536 in a child sedated with propofol. *Crit Care Med* **26**, 2087-2092 (1998).
537 11 Prabhakar, N. R. & Semenza, G. L. Adaptive and maladaptive cardiorespiratory
538 responses to continuous and intermittent hypoxia mediated by hypoxia-inducible
539 factors 1 and 2. *Physiol Rev* **92**, 967-1003, doi:10.1152/physrev.00030.2011
540 (2012).
541 12 Murphy, M. P. How mitochondria produce reactive oxygen species. *Biochem J*
542 **417**, 1-13, doi:10.1042/BJ20081386 (2009).
543 13 Chen, Q., Vazquez, E. J., Moghaddas, S., Hoppel, C. L. & Lesnefsky, E. J.
544 Production of reactive oxygen species by mitochondria: central role of complex
545 III. *J Biol Chem* **278**, 36027-36031, doi:10.1074/jbc.M304854200 (2003).
546 14 Chandel, N. S. & Schumacker, P. T. Cells depleted of mitochondrial DNA
547 (rho0) yield insight into physiological mechanisms. *FEBS Lett* **454**, 173-176
548 (1999).
549 15 Ishikawa, K. *et al.* Enhanced glycolysis induced by mtDNA mutations does not
550 regulate metastasis. *FEBS Lett* **582**, 3525-3530,
551 doi:10.1016/j.febslet.2008.09.024 (2008).
552 16 Ishikawa, K. *et al.* ROS-generating mitochondrial DNA mutations can regulate
553 tumor cell metastasis. *Science* **320**, 661-664, doi:10.1126/science.1156906
554 (2008).
555 17 Ferrannini, E. The target of metformin in type 2 diabetes. *N Engl J Med* **371**,
556 1547-1548, doi:10.1056/NEJMcibr1409796 (2014).
557 18 Wheaton, W. W. *et al.* Metformin inhibits mitochondrial complex I of cancer

558 cells to reduce tumorigenesis. *Elife* **3**, e02242, doi:10.7554/eLife.02242 (2014).
559 19 Gui, D. Y. *et al.* Environment Dictates Dependence on Mitochondrial Complex I
560 for NAD+ and Aspartate Production and Determines Cancer Cell Sensitivity to
561 Metformin. *Cell Metab* **24**, 716-727, doi:10.1016/j.cmet.2016.09.006 (2016).
562 20 Bridges, H. R., Jones, A. J., Pollak, M. N. & Hirst, J. Effects of metformin and
563 other biguanides on oxidative phosphorylation in mitochondria. *Biochem J* **462**,
564 475-487, doi:10.1042/BJ20140620 (2014).
565 21 Matsuzaki, S. & Humphries, K. M. Selective inhibition of deactivated
566 mitochondrial complex I by biguanides. *Biochemistry* **54**, 2011-2021,
567 doi:10.1021/bi501473h (2015).
568 22 Luengo, A., Sullivan, L. B. & Heiden, M. G. Understanding the complex-I-ty of
569 metformin action: limiting mitochondrial respiration to improve cancer therapy.
570 *BMC Biol* **12**, 82, doi:10.1186/s12915-014-0082-4 (2014).
571 23 Ludbrook, G. L., Visco, E. & Lam, A. M. Propofol: relation between brain
572 concentrations, electroencephalogram, middle cerebral artery blood flow
573 velocity, and cerebral oxygen extraction during induction of anesthesia.
574 *Anesthesiology* **97**, 1363-1370 (2002).
575 24 Vanlander, A. V. *et al.* Possible pathogenic mechanism of propofol infusion
576 syndrome involves coenzyme q. *Anesthesiology* **122**, 343-352,
577 doi:10.1097/ALN.0000000000000484 (2015).
578 25 Krajcova, A., Waldauf, P., Andel, M. & Duska, F. Propofol infusion syndrome:
579 a structured review of experimental studies and 153 published case reports. *Crit*
580 *Care* **19**, 398, doi:10.1186/s13054-015-1112-5 (2015).
581 26 Yang, N., Liang, Y., Yang, P., Yang, T. & Jiang, L. Propofol inhibits lung

582 cancer cell viability and induces cell apoptosis by upregulating microRNA-486
583 expression. *Braz J Med Biol Res* **50**, e5794, doi:10.1590/1414-431X20165794
584 (2017).
585 27 Konno, A. *et al.* Continuous monitoring of caspase-3 activation induced by
586 propofol in developing mouse brain. *Int J Dev Neurosci* **51**, 42-49,
587 doi:10.1016/j.ijdevneu.2016.04.007 (2016).
588 28 Meng, C. *et al.* Propofol induces proliferation partially via downregulation of
589 p53 protein and promotes migration via activation of the Nrf2 pathway in human
590 breast cancer cell line MDA-MB-231. *Oncol Rep* **37**, 841-848,
591 doi:10.3892/or.2016.5332 (2017).
592 29 Cui, W. Y., Liu, Y., Zhu, Y. Q., Song, T. & Wang, Q. S. Propofol induces
593 endoplasmic reticulum (ER) stress and apoptosis in lung cancer cell H460.
594 *Tumour Biol* **35**, 5213-5217, doi:10.1007/s13277-014-1677-7 (2014).
595 30 Kroemer, G., Dallaporta, B. & Resche-Rigon, M. The mitochondrial death/life
596 regulator in apoptosis and necrosis. *Annu Rev Physiol* **60**, 619-642,
597 doi:10.1146/annurev.physiol.60.1.619 (1998).
598 31 Kajimoto, M. *et al.* Propofol compared with isoflurane inhibits mitochondrial
599 metabolism in immature swine cerebral cortex. *J Cereb Blood Flow Metab* **34**,
600 514-521, doi:10.1038/jcbfm.2013.229 (2014).
601 32 Forkink, M. *et al.* Complex I and complex III inhibition specifically increase
602 cytosolic hydrogen peroxide levels without inducing oxidative stress in HEK293
603 cells. *Redox Biol* **6**, 607-616, doi:10.1016/j.redox.2015.09.003 (2015).
604 33 Wong, H. S., Dighe, P. A., Mezera, V., Monternier, P. A. & Brand, M. D.
605 Production of superoxide and hydrogen peroxide from specific mitochondrial

606 sites under different bioenergetic conditions. *J Biol Chem* **292**, 16804-16809,
607 doi:10.1074/jbc.R117.789271 (2017).
608 34 Brand, M. D. Mitochondrial generation of superoxide and hydrogen peroxide as
609 the source of mitochondrial redox signaling. *Free Radic Biol Med* **100**, 14-31,
610 doi:10.1016/j.freeradbiomed.2016.04.001 (2016).
611 35 Koshikawa, N., Hayashi, J., Nakagawara, A. & Takenaga, K. Reactive oxygen
612 species-generating mitochondrial DNA mutation up-regulates hypoxia-inducible
613 factor-1alpha gene transcription via phosphatidylinositol 3-kinase-Akt/protein
614 kinase C/histone deacetylase pathway. *J Biol Chem* **284**, 33185-33194,
615 doi:10.1074/jbc.M109.054221 (2009).
616 36 Cohen, P. J. Effect of anesthetics on mitochondrial function. *Anesthesiology* **39**,
617 153-164 (1973).
618 37 Ishikawa, K. & Hayashi, J. A novel function of mtDNA: its involvement in
619 metastasis. *Ann N Y Acad Sci* **1201**, 40-43, doi:10.1111/j.1749-
620 6632.2010.05616.x (2010).
621 38 El-Mir, M. Y. *et al.* Dimethylbiguanide inhibits cell respiration via an indirect
622 effect targeted on the respiratory chain complex I. *J Biol Chem* **275**, 223-228
623 (2000).
624 39 Owen, M. R., Doran, E. & Halestrap, A. P. Evidence that metformin exerts its
625 anti-diabetic effects through inhibition of complex 1 of the mitochondrial
626 respiratory chain. *Biochem J* **348 Pt 3**, 607-614 (2000).
627 40 Drahota, Z. *et al.* Biguanides inhibit complex I, II and IV of rat liver
628 mitochondria and modify their functional properties. *Physiol Res* **63**, 1-11
629 (2014).

630 41 Gottlieb, A., Duberstein, J. & Geller, A. Phenformin acidosis. *N Engl J Med*
631 **267**, 806-809, doi:10.1056/NEJM196210182671604 (1962).
632 42 Relman, A. S. Lactic acidosis and a possible new treatment. *N Engl J Med* **298**,
633 564-565, doi:10.1056/NEJM197803092981009 (1978).
634 43 Finsterer, J. & Scorza, F. A. Effects of antiepileptic drugs on mitochondrial
635 functions, morphology, kinetics, biogenesis, and survival. *Epilepsy Res* **136**, 5-
636 11, doi:10.1016/j.eplepsyres.2017.07.003 (2017).
637 44 Zhang, C. *et al.* Valproic Acid Promotes Human Glioma U87 Cells Apoptosis
638 and Inhibits Glycogen Synthase Kinase-3beta Through ERK/Akt Signaling. *Cell*
639 *Physiol Biochem* **39**, 2173-2185, doi:10.1159/000447912 (2016).
640 45 Uppala, R. *et al.* Aspirin increases mitochondrial fatty acid oxidation. *Biochem*
641 *Biophys Res Commun* **482**, 346-351, doi:10.1016/j.bbrc.2016.11.066 (2017).
642 46 Moreno-Lastres, D. *et al.* Mitochondrial complex I plays an essential role in
643 human respirasome assembly. *Cell Metab* **15**, 324-335,
644 doi:10.1016/j.cmet.2012.01.015 (2012).
645 47 Okamoto, A. *et al.* HIF-1-mediated suppression of mitochondria electron
646 transport chain function confers resistance to lidocaine-induced cell death. *Sci*
647 *Rep* **7**, 3816, doi:10.1038/s41598-017-03980-7 (2017).
648 48 Yokota, M. *et al.* Generation of trans-mitochondrial mito-mice by the
649 introduction of a pathogenic G13997A mtDNA from highly metastatic lung
650 carcinoma cells. *FEBS Lett* **584**, 3943-3948, doi:10.1016/j.febslet.2010.07.048
651 (2010).
652 49 Okamoto, A. *et al.* The antioxidant N-acetyl cysteine suppresses lidocaine-
653 induced intracellular reactive oxygen species production and cell death in

654 neuronal SH-SY5Y cells. *BMC Anesthesiol* **16**, 104, doi:10.1186/s12871-016-
655 0273-3 (2016).
656 50 Cheng, G. *et al.* Mitochondria-Targeted Analogues of Metformin Exhibit
657 Enhanced Antiproliferative and Radiosensitizing Effects in Pancreatic Cancer
658 Cells. *Cancer Res* **76**, 3904-3915, doi:10.1158/0008-5472.CAN-15-2534 (2016).
659 51 Salabei, J. K., Gibb, A. A. & Hill, B. G. Comprehensive measurement of
660 respiratory activity in permeabilized cells using extracellular flux analysis. *Nat*
661 *Protoc* **9**, 421-438, doi:10.1038/nprot.2014.018 (2014).
662

Tables

Table 1 Key Resources Table

Reagents	Source	Identifier
2,6-diisopropylphenol (propofol)	Sigma–Aldrich	D126608
2,4-diisopropylphenol	Sigma–Aldrich	557811
oligomycin	Sigma–Aldrich	O4876
carbonyl cyanide 4-(trifluoromethoxy) phenylhydrazone (FCCP)	Sigma–Aldrich	C2920
rotenone	Sigma–Aldrich	R8875
antimycin A	Sigma–Aldrich	A8674
D(−)-mannitol	Nacalai Tesque	21303-32
sucrose	Wako	196-00015
KH_2PO_4	Wako	169-04245
$MgCl_2$	Nacalai Tesque	20909-42
HEPES	Nacalai Tesque	17557-94
EGTA	Nacalai Tesque	37346-05
albumin from bovine serum, fatty acid-free	Wako	017-15141
sodium pyruvate	Nacalai Tesque	06977-34
L(−)-malic acid	Nacalai Tesque	21030-44
ADP, monopotassium salt	Wako	303-50751
Seahorse XF Plasma Membrane Permeabilizer	Agilent Technologies	102504-100
succinic acid, disodium salt	Nacalai Tesque	32405-62
tetramethylhydroquinone (duroquinol)	Tokyo Chemical Industry	T0822
N,N,N′,N′-tetramethyl-*p*-phenylenediamine	Wako	203-12821
L(+)-ascorbic acid, sodium salt	Nacalai Tesque	03422-32

669
670 Table 2 Identification of pathogenic mutations in mtDNA sequences
671

Position	Gene	Amino acid change	Mouse strain	Cell lines		
			C57BL/6	P29	A11	B82M
T6589C	*COI*	V421A	T	T	T	C
G9348A	*COIII*	V281I	G	G	G	A
13885insC	*ND6*	Flame-shift	-	-	-	C
G13997A	*ND6*	P25L	G	G	A	G

672
673 The G13997A mutation in *ND6* is a missense mutation that changes the amino acid
674 proline to leucine at a site that is highly conserved throughout vertebrates. The
675 13885insC mutation in *ND6* is a frameshift mutation that has been previously reported
676 as a pathogenic mutation inducing substantial complex I defects in some sublines of the
677 L929 fibroblast cell line.
678 Bases: A, Adenine; G, Guanine; C, Cytosine; T: Thymine
679 Amino acids: V, Valine; A, Alanine; I, Isoleucine; P, Proline; L, Leucine
680

681
682 Table 3 Genetic characteristics of parent cells and their transmitochondrial cybrids
683

Cell lines	Nuclear genotype	Fusion combinations	
		Nuclear donor	mtDNA donors
ρ0P29	P29	ρ0P29	(−)
P29mtA11	P29	ρ0P29	enA11
P29mtB82M	P29	ρ0P29	enB82M
P29mtCOIM	P29	ρ0P29	enB82
P29mtΔ	P29	ρ0P29	enB82mtΔ

684

685 ρ0, mtDNA-less cells; en, enucleated donor.

686

687 Figure Legends

688 **Figure 1 Propofol induced cell death in a concentration- and time-dependent**
689 **manner**

690 SH-SY5Y cells were exposed to the indicated concentrations (12.5, 25, 50, 100, and
691 150 μM) of propofol for 6 h (a and b) and 3, 6, and 12 h (c). Cells were harvested, and
692 percentages of cell death were measured by flow cytometry. The ratio of PI-positive
693 and/or annexin V-positive cells [(Q1 + Q2 + Q4)/(Q1 + Q2 + Q3 + Q4)] was used to
694 calculate the percentage of dead cells (a and b) (n = 3). Data presented in (b and c) are
695 expressed as the mean ± SD. Differences between treatment groups were evaluated by
696 one-way ANOVA, followed by Dunnett's multiple comparison test (b), or by two-way
697 ANOVA, followed by Dunnett's multiple comparison test (c). *$p < 0.05$ compared to
698 the control cell population (incubation for 0 h, no treatment).

699

700 **Figure 2 Propofol induced caspase activation in a concentration- and time-**
701 **dependent manner**

702 SH-SY5Y cells were exposed to the indicated concentrations (12.5, 25, 50, 100, and
703 150 μM) of propofol for 6 h (a and b) and 3, 6, and 12 h (c). Caspase-9 (n = 5) (a) and
704 caspase-3/7 (n = 5) (b and c) activities in each treatment group at different time points.
705 (d) SH-SY5Y cells were exposed to the indicated concentrations (12.5, 25, 50, 100, and
706 150 μM) of propofol for 6 and 12 h. The levels of LDH activity were assayed in culture
707 supernatants (n = 3). Treatment with lysis buffer served as a control. (e) Average
708 mitochondrial membrane potential (ΔΨm) of untreated cells and cells treated with the
709 indicated concentrations (25, 50, and 100 μM) of propofol (n = 3) for 6 h. Values
710 indicate the ratio [Q2/(Q2 + Q4)] of green JC-1 monomers (527 nm emission) to red

711 aggregates (590 nm emission). Data presented in (a–g) are expressed as the mean ± SD.
712 Differences between treatment groups were evaluated by one-way ANOVA, followed
713 by Dunnett's multiple comparison test (a, b, and e), or by two-way ANOVA, followed
714 by Dunnett's multiple comparison test (c and d). *$p < 0.05$ compared to the control cell
715 population (incubation for 0 h, no treatment).
716
717 **Figure 3 Oxygen metabolism and ROS generation in SH-SY5Y cells treated with**
718 **propofol**
719 OCR (a, b, and e) and ECAR (c, d, and f) in SH-SY5Y cells exposed to the indicated
720 concentrations of propofol (12.5, 25, 50, and 100 μM) for 6 h (b and d) or 0, 3, 6, and
721 12 h (e and f). Data presented in (b, d–f) are expressed as the means ± SD. Differences
722 between treatment groups were evaluated by one-way ANOVA, followed by Dunnett's
723 multiple comparison test (b and d), or by two-way ANOVA, followed by Dunnett's
724 multiple comparison test (e and f). (g) ROS production in SH-SY5Y cells exposed to
725 25, 50, and 100 μM propofol (n = 3) for 3 h. (h) SH-SY5Y cells were exposed to the
726 indicated concentrations (50 and 100 μM) of propofol for 6 h with or without treatment
727 with 10 mM *N*-acetylcysteine. Cells were harvested, and percentages of cell death were
728 measured by flow cytometry. MFI: median fluorescence intensity; NAC: *N*-
729 acetylcysteine. *$p < 0.05$ compared to the control cell population.
730
731 **Figure 4 Involvement of functional mitochondria in propofol-induced caspase**
732 **activation and cell death**
733 P29 cells and cells of the ρ0P29 derivative lacking mtDNA were exposed to the
734 indicated concentrations (25 and 50 μM) of propofol for 6 h. (a) Cells were harvested,

735 and percentages of cell death were measured by flow cytometry. The ratio of PI-positive
736 and/or annexin V-positive cells [(Q1 + Q2 + Q4)/(Q1 + Q2 + Q3 + Q4)] was used to
737 calculate the percentage of dead cells (Supplementary Fig. 1a) (n = 3). (b) Caspase-3/7
738 activity in each treatment group (n = 3) at 6 h. Differences between treatment groups
739 were evaluated by one-way ANOVA, followed by Dunnett's multiple comparison test.
740 *$p < 0.05$ compared to the control cell population; #$p < 0.05$ compared to the indicated
741 experimental groups.
742
743 **Figure 5 Effects of propofol on OCR driven by each complex of the mitochondrial**
744 **electron transport chain**
745 Representative OCR traces of mitochondrial respiration using protocol A
746 (Supplementary Fig. 4a) and protocol B (Supplementary Fig. 4b). Mitochondrial ETC-
747 mediated OCR, driven by complexes I (c), II (d), III (e), and IV (f), were assayed by a
748 flux analyzer-based protocol. SH-SY5Y cells were exposed to 100 and 200 μM
749 propofol for 6 h and subjected to the assay. Differences between treatment groups were
750 evaluated by one-way ANOVA, followed by Dunnett's multiple comparison test. *$p <$
751 0.05 compared to the control cell population.
752
753 **Figure 6 Synergistic effects of propofol and mitochondrial ETC inhibitors on**
754 **caspase activity and cell death**
755 Levels of caspase-3/7 activity and cell death of SH-SY5Y cells treated with propofol
756 and mitochondrial ETC inhibitors. Cells were treated with 12.5, 25, or 50 μM propofol
757 and with either 100 nM rotenone, 4 μM oligomycin, or 25 μg/mL antimycin A and
758 subjected to (a) a cell death assay and (b) a caspase-3/7 activity assay (n = 3).

759 Percentages of cell death were measured by flow cytometry. The ratio of PI-positive
760 and/or annexin V-positive cells [(Q1 + Q2 + Q4)/(Q1 + Q2 + Q3 + Q4)] was used to
761 calculate the percentage of dead cells (Supplementary Fig. 1a) (n = 3). All data are
762 expressed as the means ± SD. *$p < 0.05$ compared with control cells (no treatment); #p
763 < 0.05 compared with the indicated groups. rot: rotenone; olig: oligomycin; anti:
764 antimycin A.
765
766 **Figure 7 Effects of propofol on caspase activity and cell death in various**
767 **transmitochondrial cybrid cells**
768 (a) OCR and (b) ECAR of P29, its cybrid cells, and ρ0 cells. (c and d) P29, its cybrid
769 cells, and ρ0 cells were exposed to the indicated concentrations (12.5, 25, and 50 μM)
770 of propofol for 6 h. Cells were harvested, and percentages of cell death were measured
771 by flow cytometry. The ratio of PI-positive and/or annexin V-positive cells [(Q1 + Q2 +
772 Q4)/(Q1 + Q2 + Q3 + Q4)] was used to calculate the percentage of dead cells (n = 3)
773 (c). Caspase-3/7 activity in each treatment group (n = 3) at 6 h (d). (e) P29, P29mtA11
774 and ρ0 cells were exposed to 25 and 50 μM propofol for 6 h and subjected to ROS
775 assay. (f) P29mtA11 cells were exposed to 25 μM propofol with or without 10 mM
776 NAC for 6 h. Cells were harvested, and percentages of cell death were measured by
777 flow cytometry. Data presented in (a–f) are expressed as the means ± SD. Differences
778 between treatment groups were evaluated by one-way ANOVA, followed by Dunnett's
779 multiple comparison test (a, b, e and f) or by two-way ANOVA, followed by Dunnett's
780 multiple comparison test (c and d). *$p < 0.05$ compared to the control cell population.
781 A11: P29mtA11 cells; B82M: P29mtB82M cells; COIM: P29mtCOIM cells; mtΔ:
782 P29mtΔ cells.

783

784 **Figure 8 Synergistic effects of propofol and metformin on caspase activity and cell**

785 **death**

786 (a) OCR and (b) ECAR of SH-SY5Y cells exposed to the indicated concentrations of

787 metformin (2.5, 5, 10, and 20 mM) for 6 h. (c) SH-SY5Y cells were exposed to 25 μM

788 propofol with or without 5 mM metformin, and ROS production was determined (n =

789 3). (d and e) SH-SY5Y cells were exposed to the indicated concentrations (12.5, 25, 50,

790 and 100 μM) of propofol with or without 5 mM metformin for 6 h. (d) Cells were

791 harvested, and percentages of cell death were measured by flow cytometry. The ratio of

792 PI-positive and/or annexin V-positive cells [(Q1 + Q2 + Q4)/(Q1 + Q2 + Q3 + Q4)] was

793 used to calculate the percentage of dead cells (n = 3). (e) Caspase-3/7 activity in each

794 treatment group (n = 3). Data presented in (a–e) are expressed as the means ± SD.

795 Differences between treatment groups were evaluated by one-way ANOVA, followed

796 by Dunnett's multiple comparison test (a, b, and c), or by two-way ANOVA, followed

797 by Dunnett's multiple comparison test (d and e). *$p < 0.05$ compared to the control cell

798 population; #$p < 0.05$ compared to the indicated experimental groups.

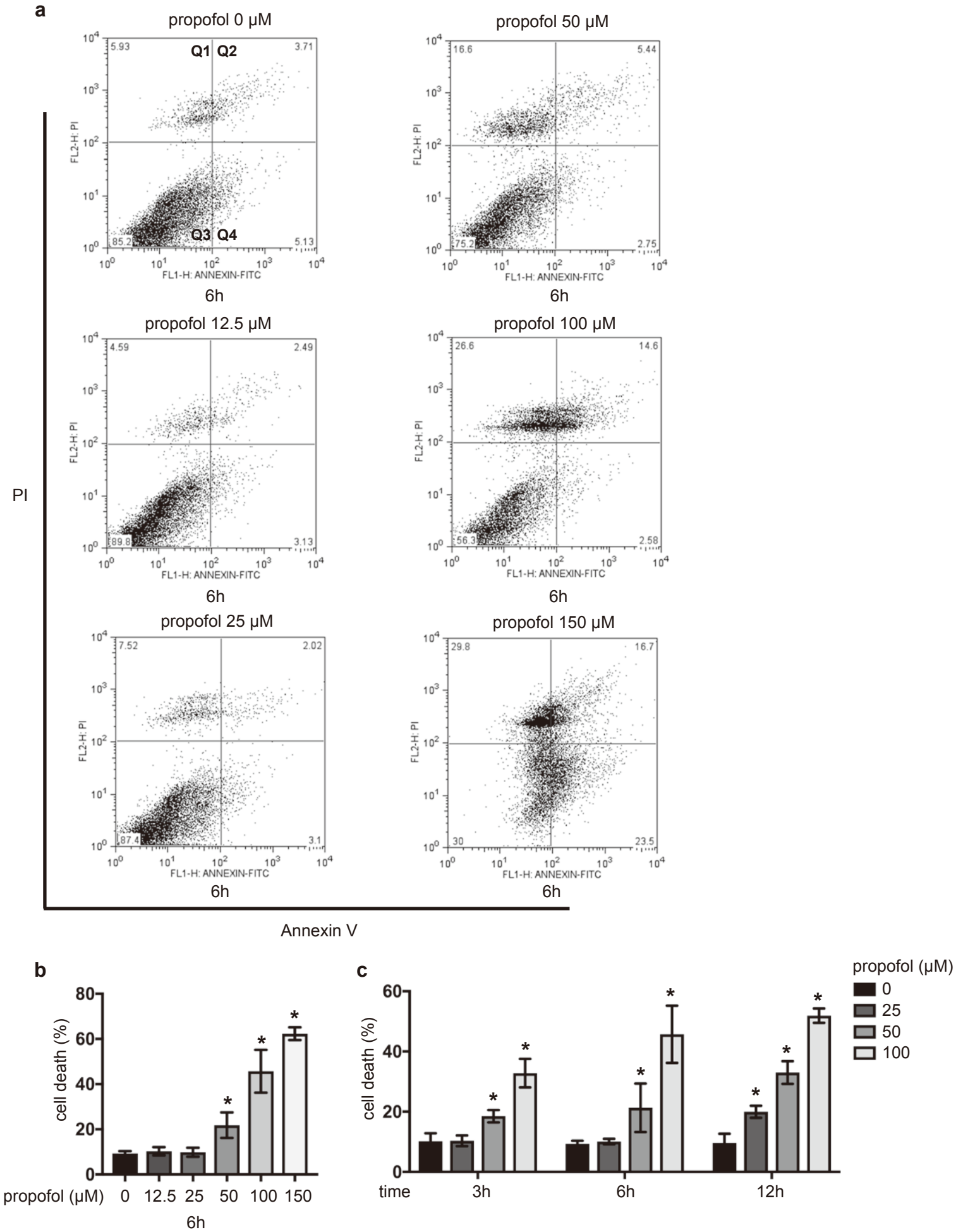
a
propofol 0 μM
5.93
Q1
Q2
3.71
Q3
Q4
85.2
5.13
propofol 50 μM
16.6
5.44
75.2
2.75
propofol 12.5 μM
4.59
2.49
89.8
3.13
propofol 100 μM
26.6
14.6
56.3
2.58
propofol 25 μM
7.52
2.02
87.4
3.1
propofol 150 μM
29.8
16.7
30
23.5
FL1-H: ANNEXIN-FITC
FL2-H: PI
6h
PI
Annexin V
b
cell death (%)
propofol (μM)
0
12.5
25
50
100
150
6h
c
cell death (%)
time
3h
6h
12h
propofol (μM)
0
25
50
100

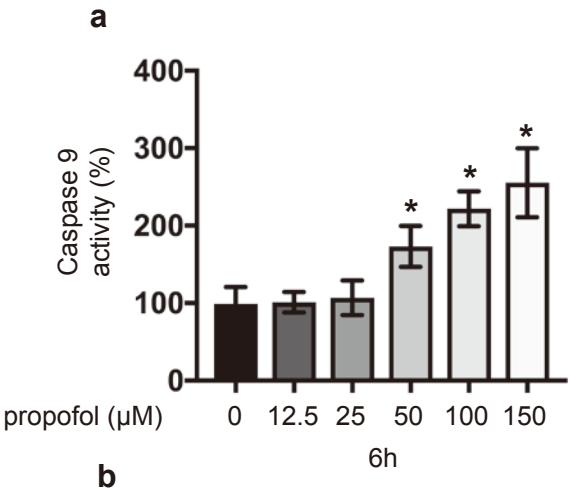
a
Caspase 9 activity (%)
400
300
200
100
0
propofol (μM)
0
12.5
25
50
100
150
6h

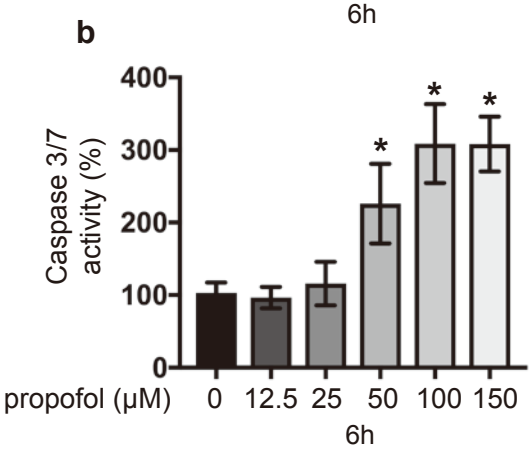
b
Caspase 3/7 activity (%)
400
300
200
100
0
propofol (μM)
0
12.5
25
50
100
150
6h

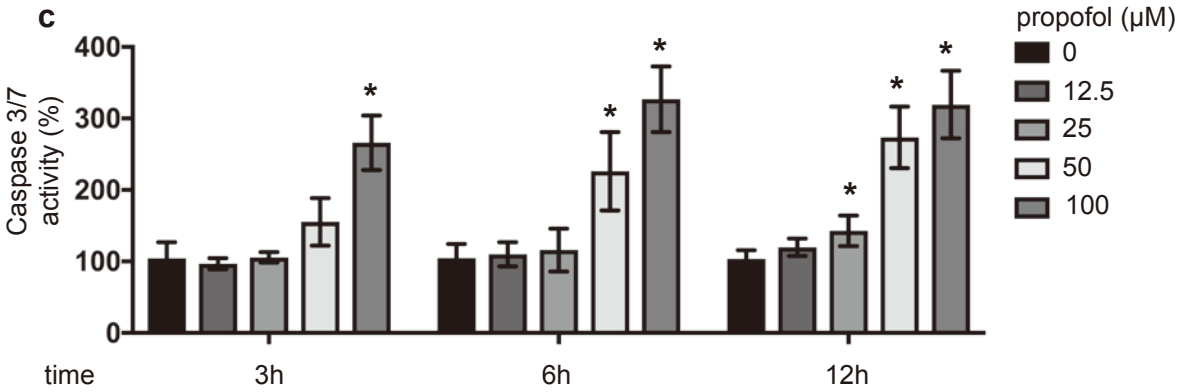
c
Caspase 3/7 activity (%)
400
300
200
100
0
time
3h
6h
12h
propofol (μM)
0
12.5
25
50
100

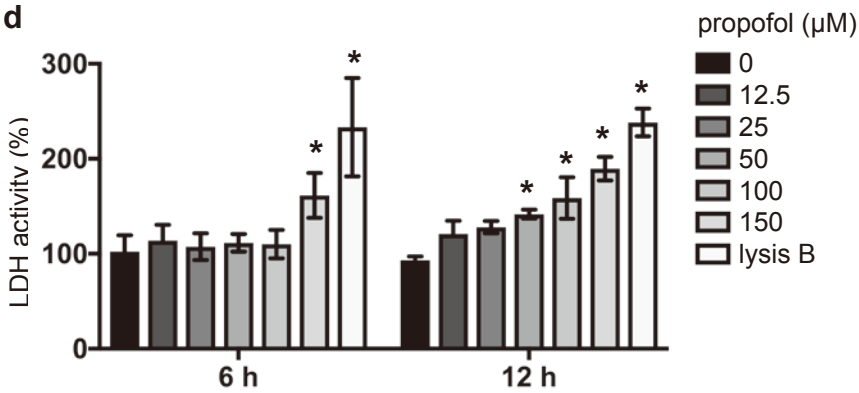
d
LDH activity (%)
300
200
100
0
6 h
12 h
propofol (μM)
0
12.5
25
50
100
150
lysis B

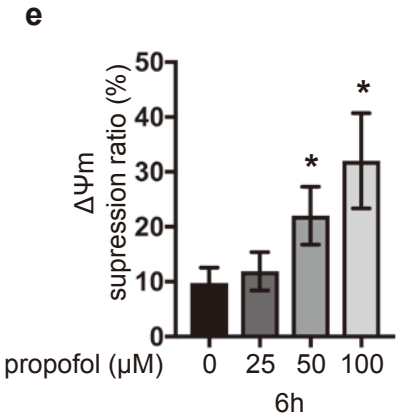
e
ΔΨm supression ratio (%)
50
40
30
20
10
0
propofol (μM)
0
25
50
100
6h

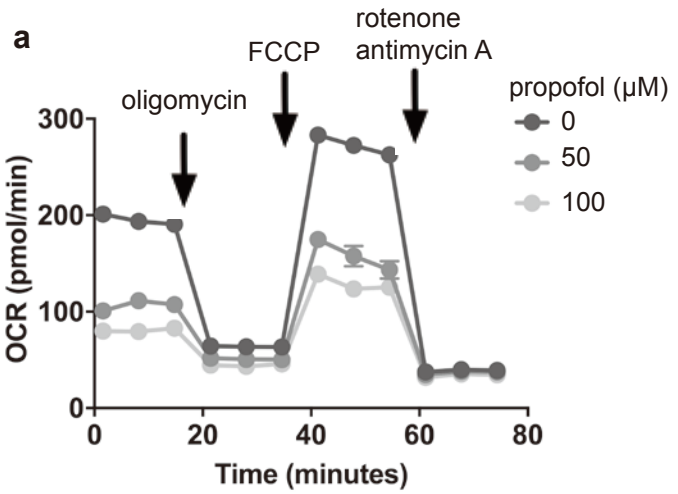
a
oligomycin
FCCP
rotenone
antimycin A
propofol (μM)
0
50
100
OCR (pmol/min)
Time (minutes)

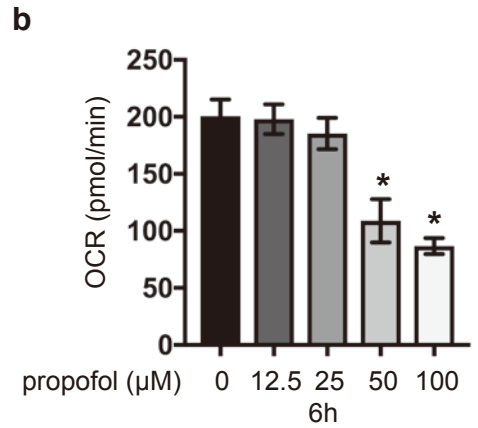
b
OCR (pmol/min)
propofol (μM) 0 12.5 25 50 100
6h

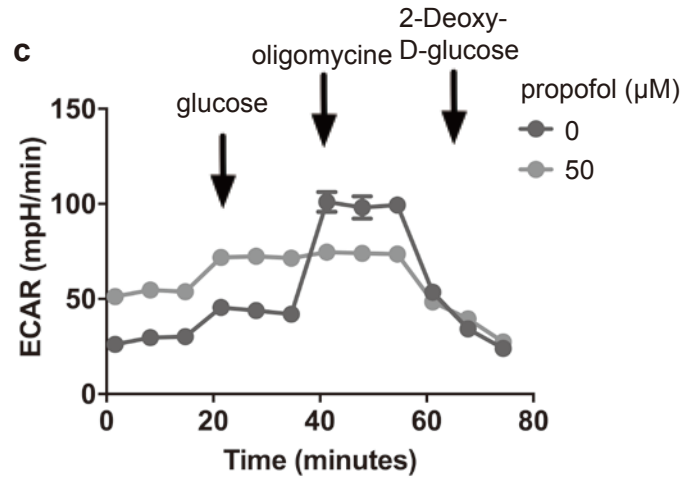
c
glucose
oligomycine
2-Deoxy-
D-glucose
propofol (μM)
0
50
ECAR (mpH/min)
Time (minutes)

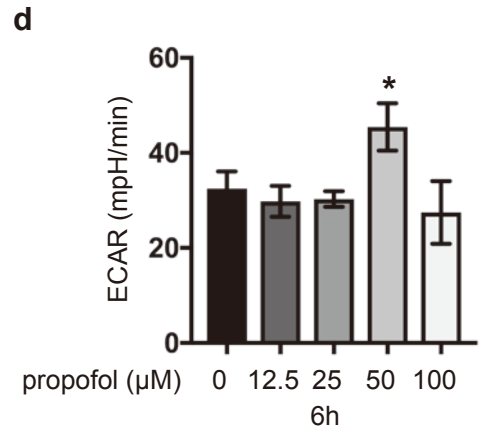
d
ECAR (mpH/min)
propofol (μM) 0 12.5 25 50 100
6h

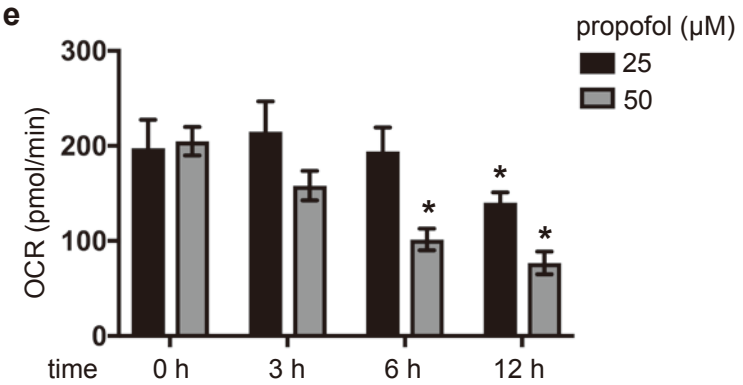
e
propofol (μM)
25
50
OCR (pmol/min)
time 0 h 3 h 6 h 12 h

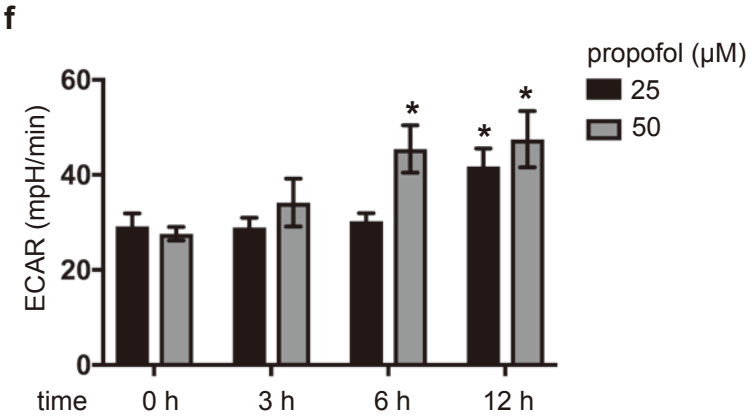
f
propofol (μM)
25
50
ECAR (mpH/min)
time 0 h 3 h 6 h 12 h

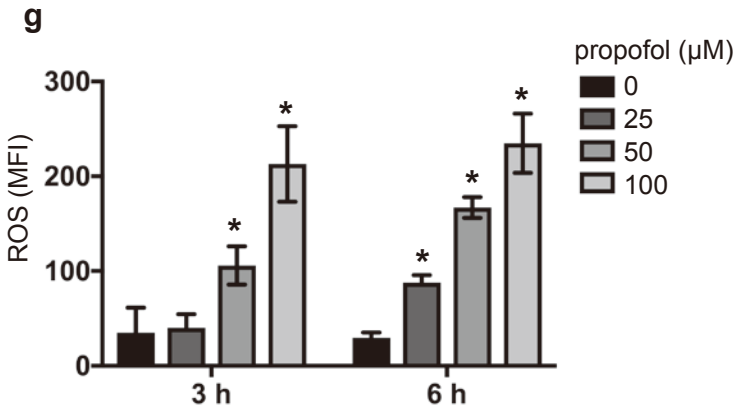
g
propofol (μM)
0
25
50
100
ROS (MFI)
3 h
6 h

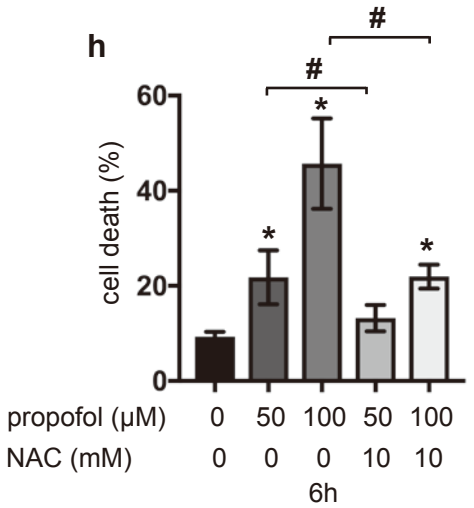
h
#
#
cell death (%)
propofol (μM) 0 50 100 50 100
NAC (mM) 0 0 0 10 10
6h

a

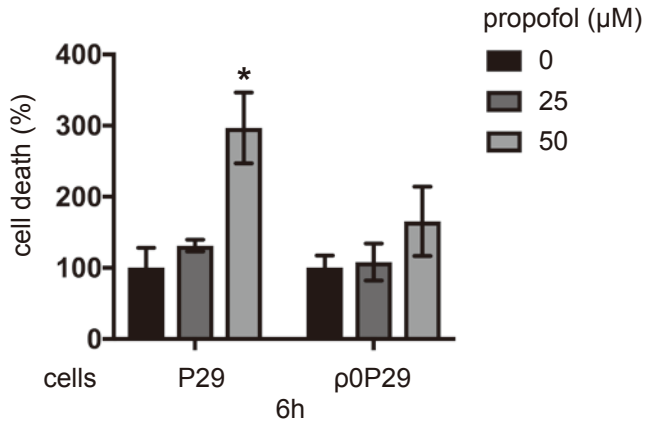
propofol (μM)
0
25
50
cell death (%)
400
300
200
100
0
*
cells
P29
ρ0P29
6h

b

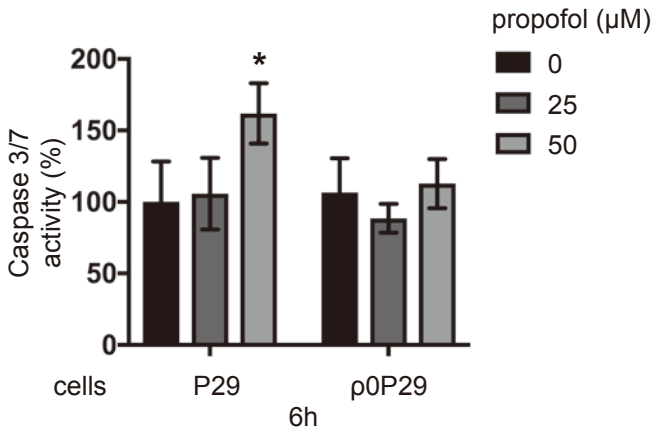
propofol (μM)
0
25
50
Caspase 3/7 activity (%)
200
150
100
50
0
*
cells
P29
ρ0P29
6h

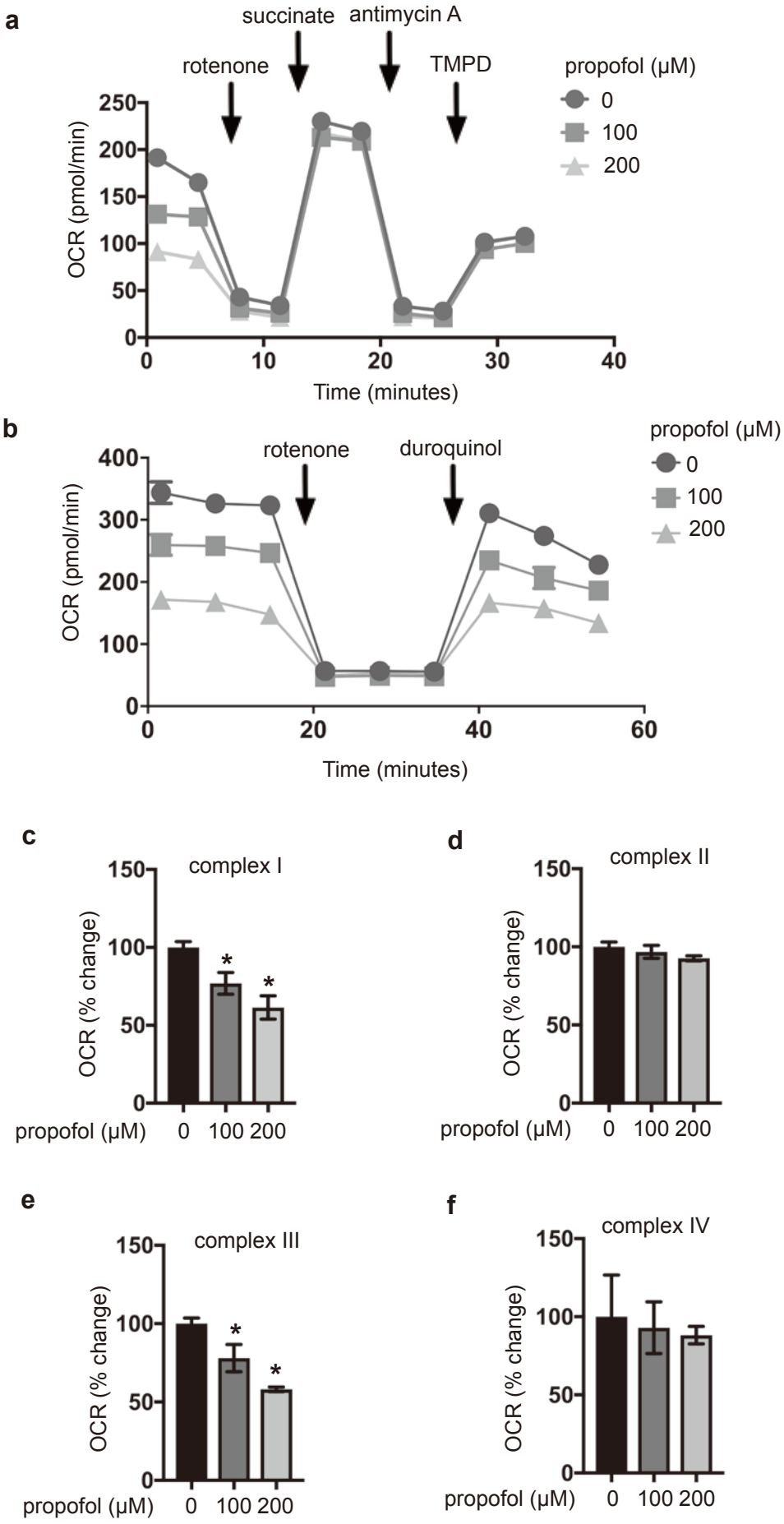
a
succinate
antimycin A
rotenone
TMPD
propofol (μM)
0
100
200
OCR (pmol/min)
Time (minutes)
b
rotenone
duroquinol
propofol (μM)
0
100
200
OCR (pmol/min)
Time (minutes)
c
complex I
OCR (% change)
propofol (μM) 0 100 200
d
complex II
OCR (% change)
propofol (μM) 0 100 200
e
complex III
OCR (% change)
propofol (μM) 0 100 200
f
complex IV
OCR (% change)
propofol (μM) 0 100 200

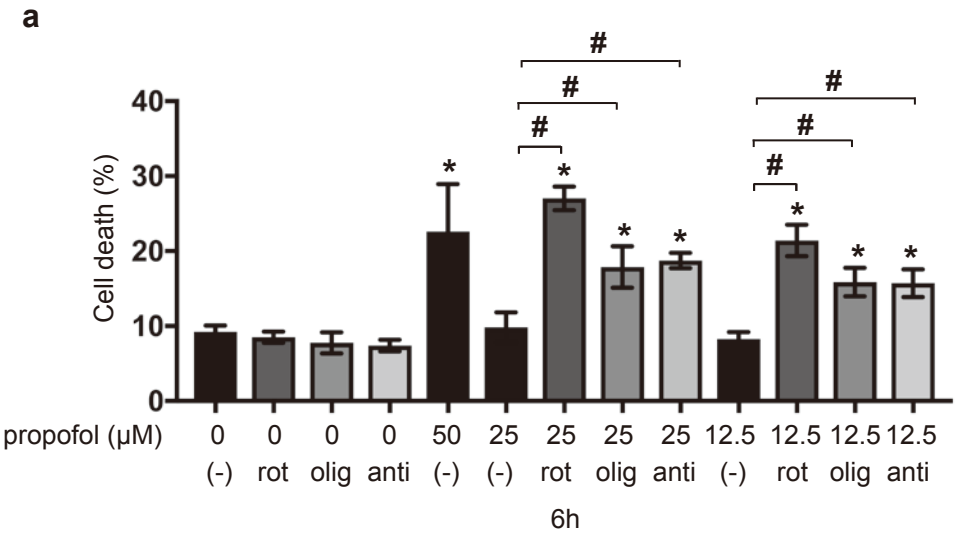
a
Cell death (%)
40
30
20
10
0
propofol (μM)
0 (-)
0 rot
0 olig
0 anti
50 (-)
25 (-)
25 rot
25 olig
25 anti
12.5 (-)
12.5 rot
12.5 olig
12.5 anti
6h
#
*

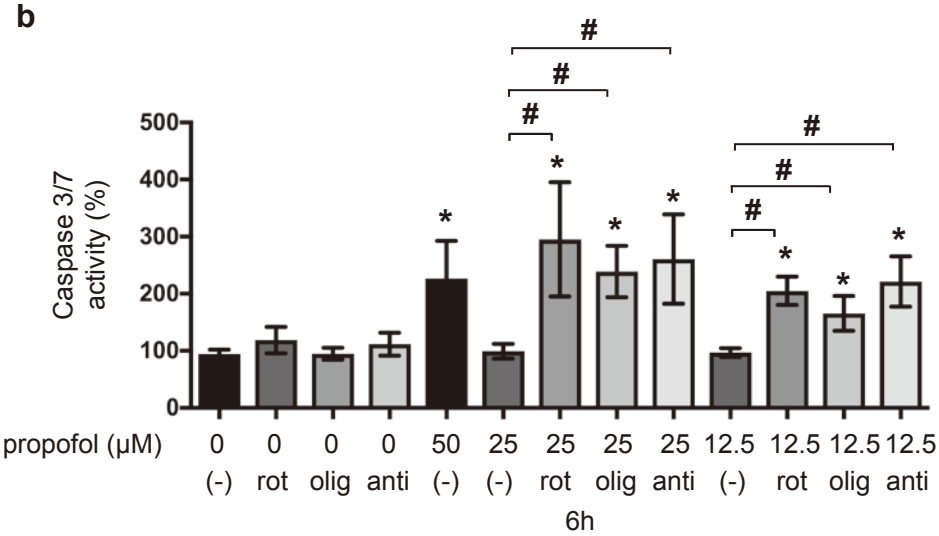
b
Caspase 3/7 activity (%)
500
400
300
200
100
0
propofol (μM)
0 (-)
0 rot
0 olig
0 anti
50 (-)
25 (-)
25 rot
25 olig
25 anti
12.5 (-)
12.5 rot
12.5 olig
12.5 anti
6h
#
*

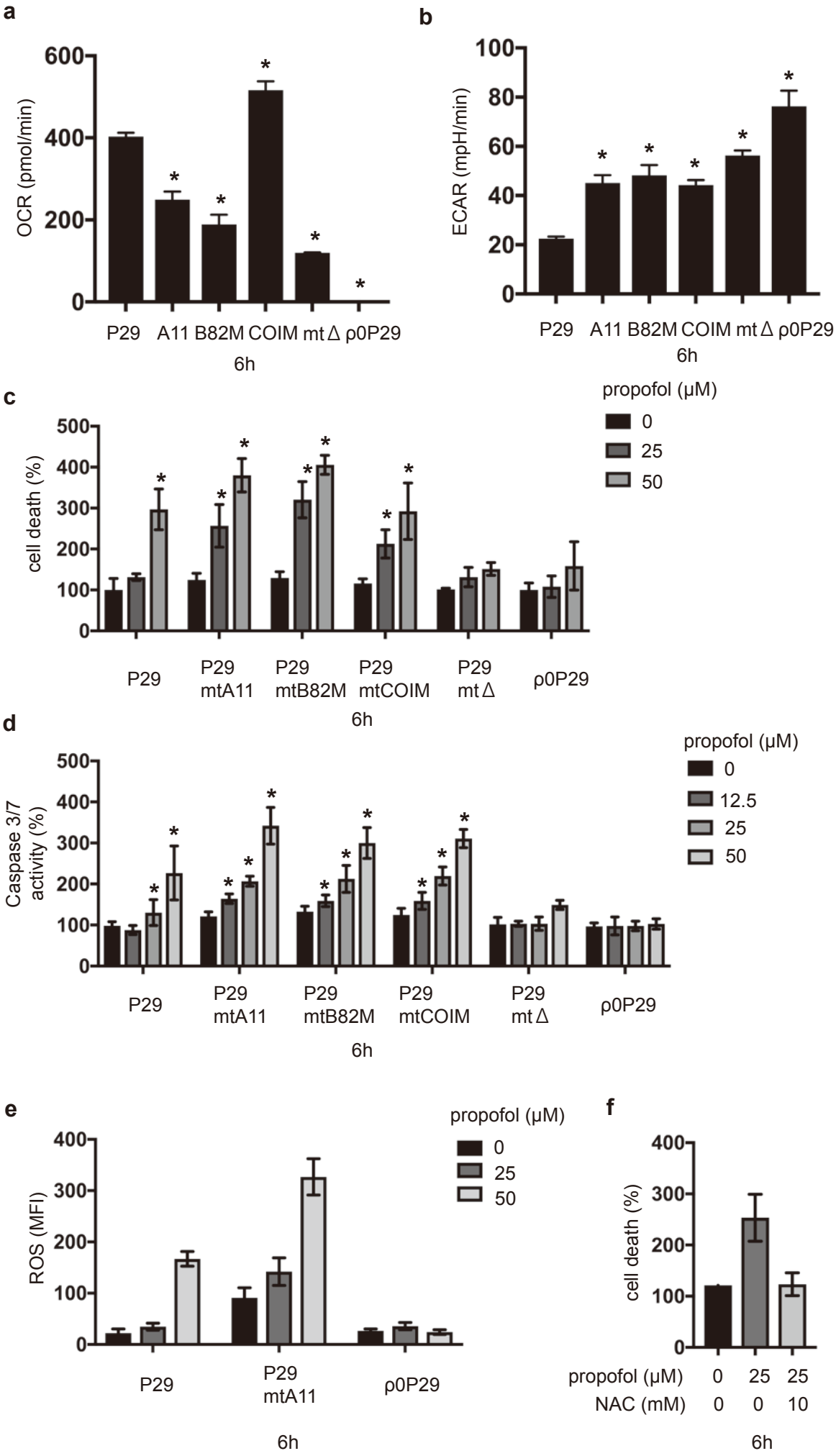
a
OCR (pmol/min)
600
400
200
0
P29
A11
B82M
COIM
mtΔ
ρ0P29
6h
b
ECAR (mpH/min)
100
80
60
40
20
0
P29
A11
B82M
COIM
mtΔ
ρ0P29
6h
c
cell death (%)
500
400
300
200
100
0
P29
P29 mtA11
P29 mtB82M
P29 mtCOIM
P29 mtΔ
ρ0P29
6h
propofol (μM)
0
25
50
d
Caspase 3/7 activity (%)
500
400
300
200
100
0
P29
P29 mtA11
P29 mtB82M
P29 mtCOIM
P29 mtΔ
ρ0P29
6h
propofol (μM)
0
12.5
25
50
e
ROS (MFI)
400
300
200
100
0
P29
P29 mtA11
ρ0P29
6h
propofol (μM)
0
25
50
f
cell death (%)
400
300
200
100
0
propofol (μM) 0 25 25
NAC (mM) 0 0 10
6h

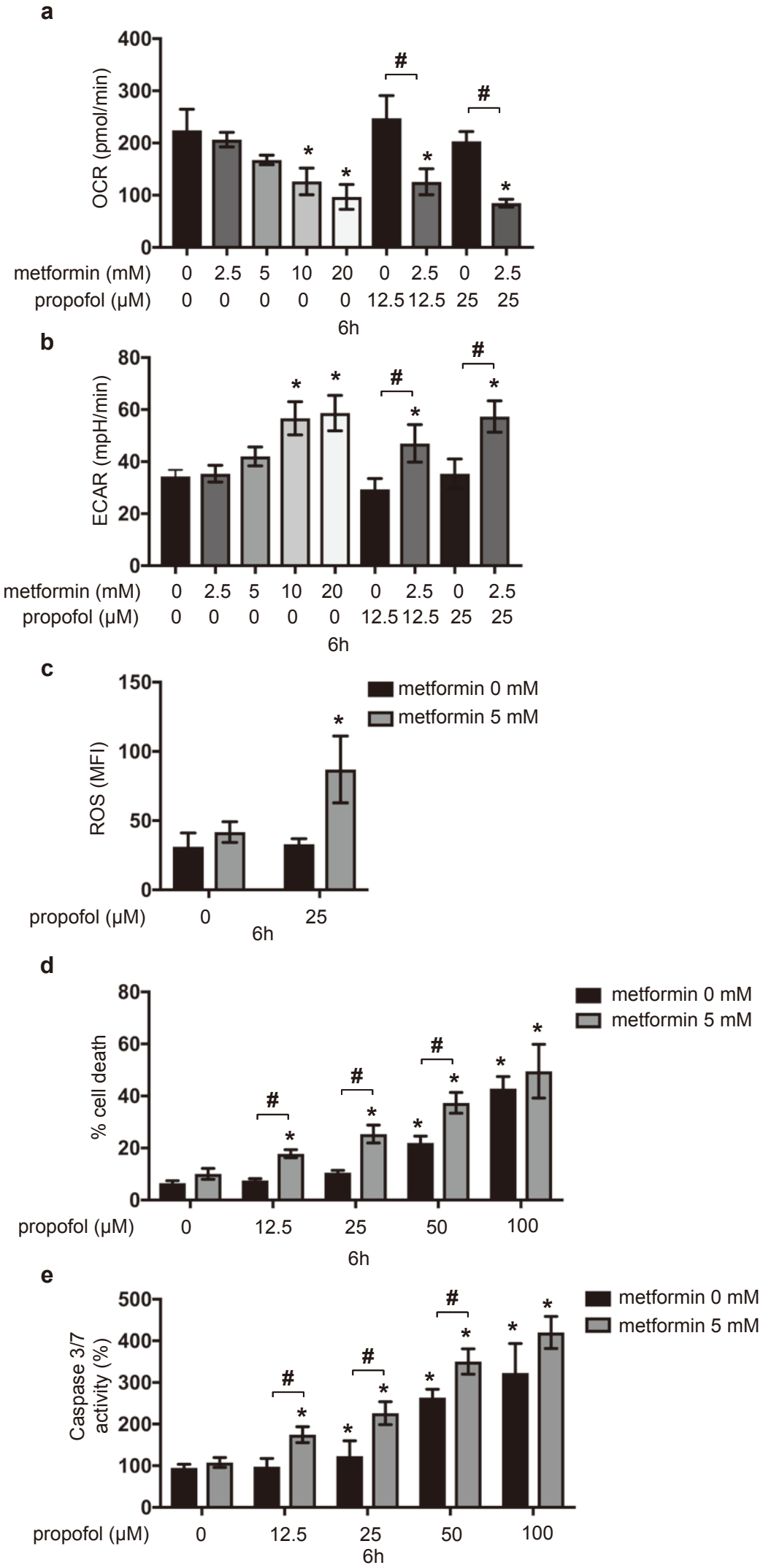
a
OCR (pmol/min)
400
300
200
100
0
metformin (mM) 0 2.5 5 10 20 0 2.5 0 2.5
propofol (μM) 0 0 0 0 0 12.5 12.5 25 25
6h
b
ECAR (mpH/min)
80
60
40
20
0
metformin (mM) 0 2.5 5 10 20 0 2.5 0 2.5
propofol (μM) 0 0 0 0 0 12.5 12.5 25 25
6h
c
ROS (MFI)
150
100
50
0
metformin 0 mM
metformin 5 mM
propofol (μM) 0 25
6h
d
% cell death
80
60
40
20
0
metformin 0 mM
metformin 5 mM
propofol (μM) 0 12.5 25 50 100
6h
e
Caspase 3/7 activity (%)
500
400
300
200
100
0
metformin 0 mM
metformin 5 mM
propofol (μM) 0 12.5 25 50 100
6h

Supplementary Information

Propofol induces metabolic reprogramming and cell death in a mitochondrial electron transport chain-dependent manner

Chisato Sumi[1,2], Akihisa Okamoto[2], Masahiro Tanaka[2], Kenichiro Nishi[2], Munenori Kusunoki[1,2], Tomohiro Shoji[1,2], Takeo Uba[1,2], Yoshiyuki Matsuo[2], Takehiko Adachi[3], Keizo Takenaga[4] and Kiichi Hirota[2]

[1] Department of Anesthesiology, Kansai Medical University, Hirakata, Japan, [2] Department of Human Stress Response Science, Institute of Biomedical Science, Kansai Medical University, Hirakata, Japan, [3] Department of Anesthesiology, Tazuke Kofukai Medical Institute, Osaka, Japan, [4] Department of Life Science, Shimane University Faculty of Medicine, Izumo, Japan

Supplementary Figure 1

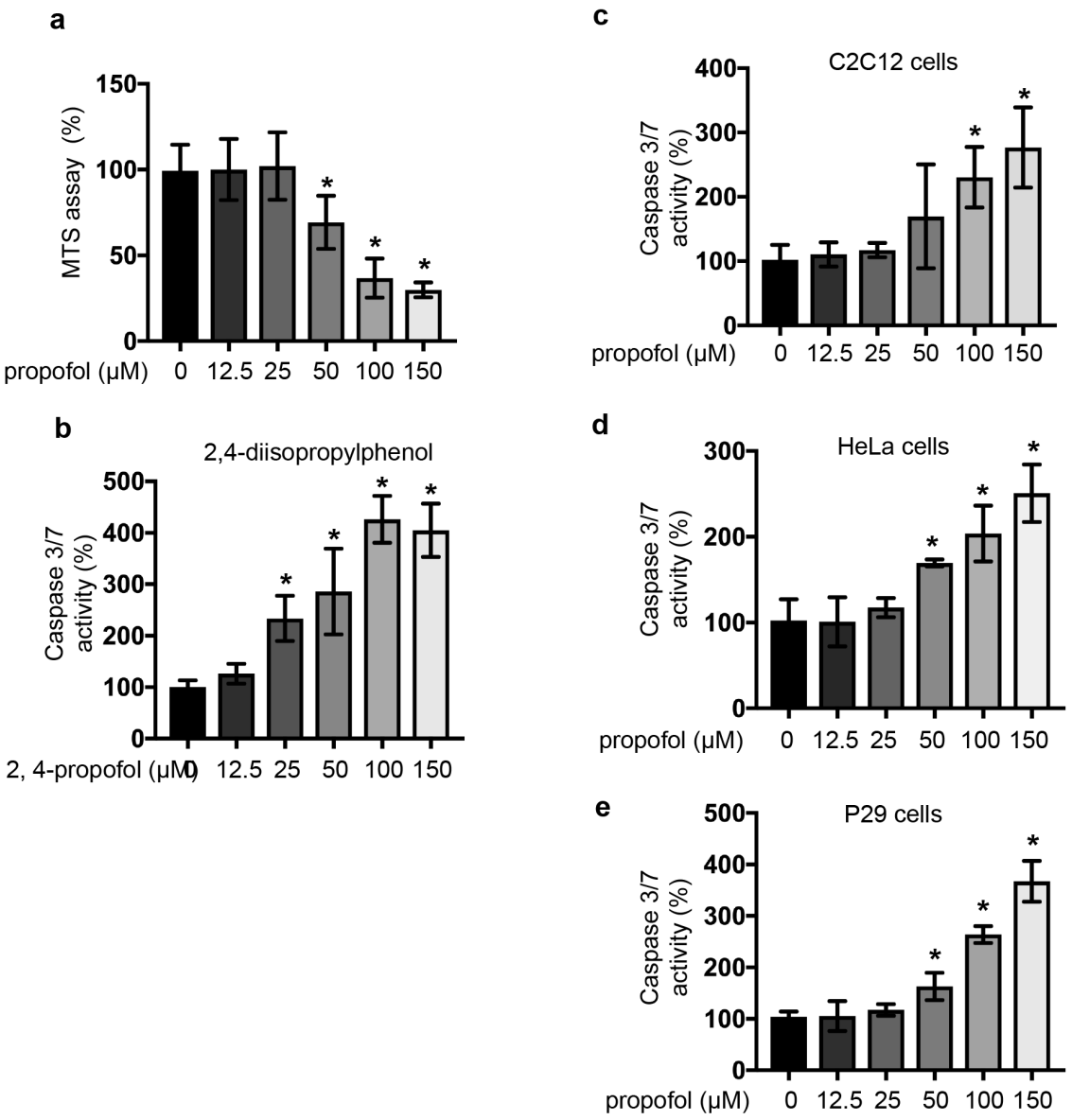

Supplementary Figure 1 | Analysis of cell proliferation, caspase 3/7 activity

(a) SH-SY5Y cells were exposed to the indicated concentrations (12.5, 25, 50, 100 or 150 μM) of propofol for 6 h. Graphic depiction of the levels of cell proliferation of treated and untreated cells, as evaluated by MTS [3-(4,5-dimethylthiazol-2-yl)-5-(3-carboxymethoxyphenyl)-2-(4-sulfophenyl)-2H-tetrazolium] assay (n = 3) as described in Cell growth MTS assay section in Materials and Methods section. (b) SH-SY5Y cells were exposed to the indicated concentrations (12.5, 25, 50, 100 and 150 μM) of 2,4 diisopropylphenol 6 h. Graphic depictions of caspase-3/7 (n = 3). (c, d and e) C2C12 cells (c), HeLa cells (d) and P29 cells (e) were exposed to the indicated concentrations (12.5, 25, 50, 100 and 150 μM) of propofol for 6 h. Graphic depictions of caspase-3/7 activity (n = 3). Differences between treatment groups were evaluated by one-way ANOVA, followed by Dunnett's multiple comparison test. *$p < 0.05$ compared to the control cell population (incubation for 0 h, no treatment).

Supplementary Figure 2

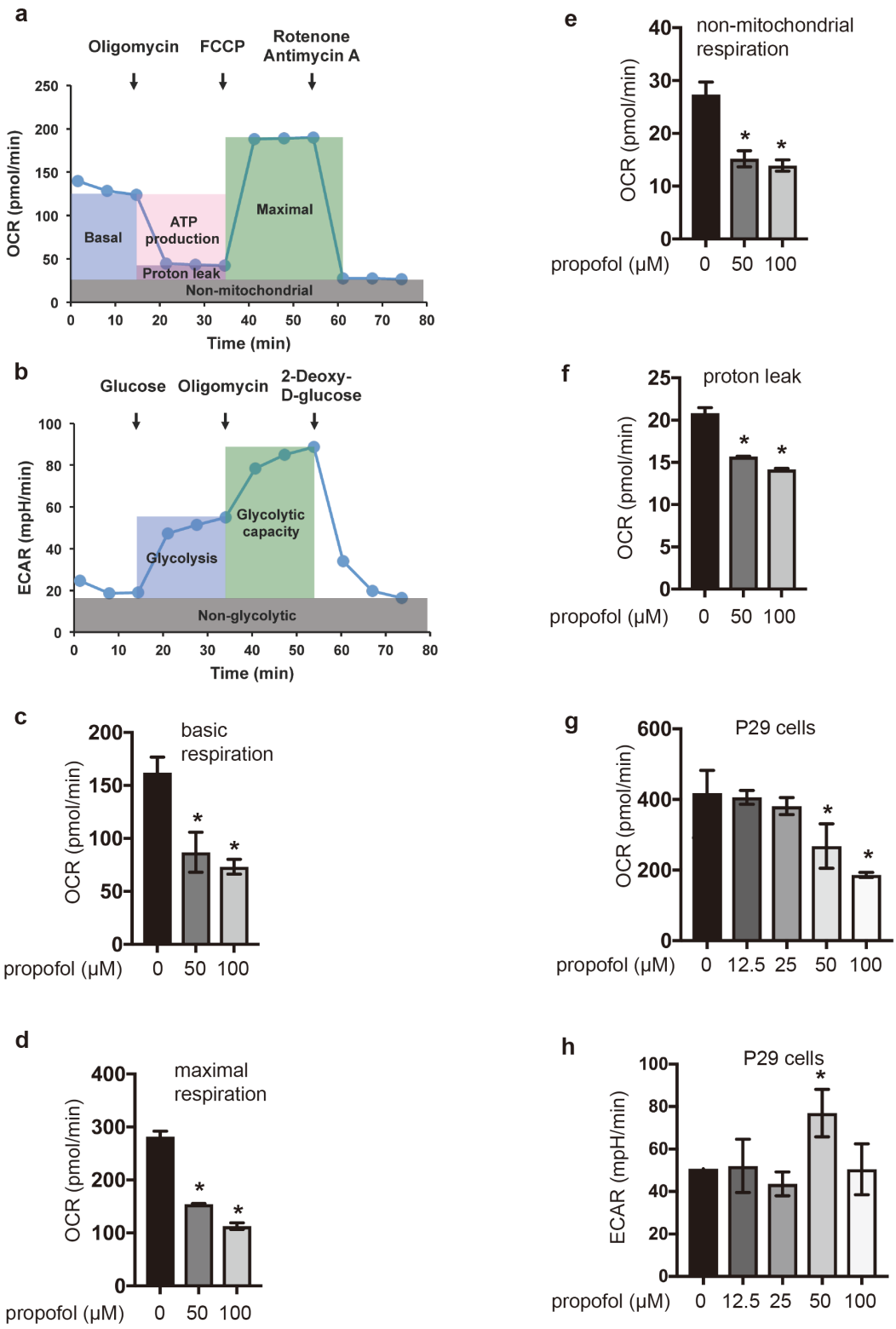

Supplementary Figure 2 | Oxygen metabolism and ROS generation in SH-SY5Y cells treated with propofol

(a) Cell Mito Stress test profile of the key parameters of mitochondrial oxygen consumption rate (OCR). (b) Cell glycolysis test profile of the key parameters of the extracellular acidification rate (ECAR). (c, d, e and f) Sequential compound injections measure basal respiration, maximal respiration, and non-mitochondrial respiration, non-mitochondrial repiration and proton leak were demonsrated. OCR (basal respiration) (c) OCR (maximal respiration) (d), OCR (non-mitochondrial respiration) (e) and Proton Leak (f) in SH-SY5Y cells treated with indicated doses of propofol were demonstrated. (g and h) OCR (f) and ECAR (h) in P29 cells exposed to the indicated doses of propofol (12.5, 25, 50 and 100 μM) for 6h. Data presented are expressed as means ± standard deviations (SD). Differences between results were evaluated by the one-way ANOVA followed by Dunnett's multiple comparison test $*p < 0.05$ compared to the control cell population.

Supplementary Figure 3

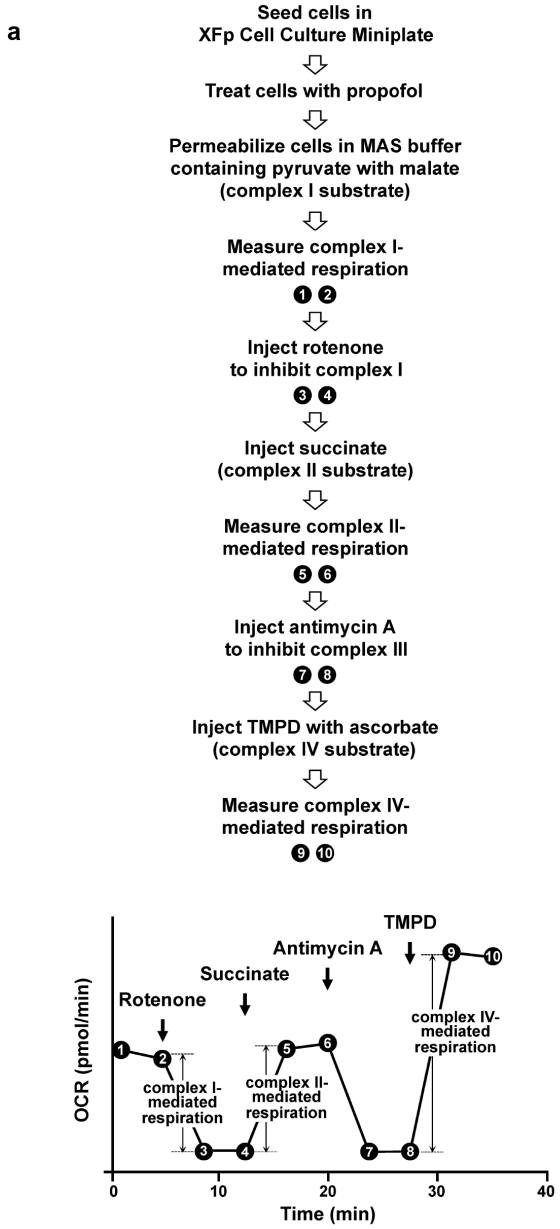

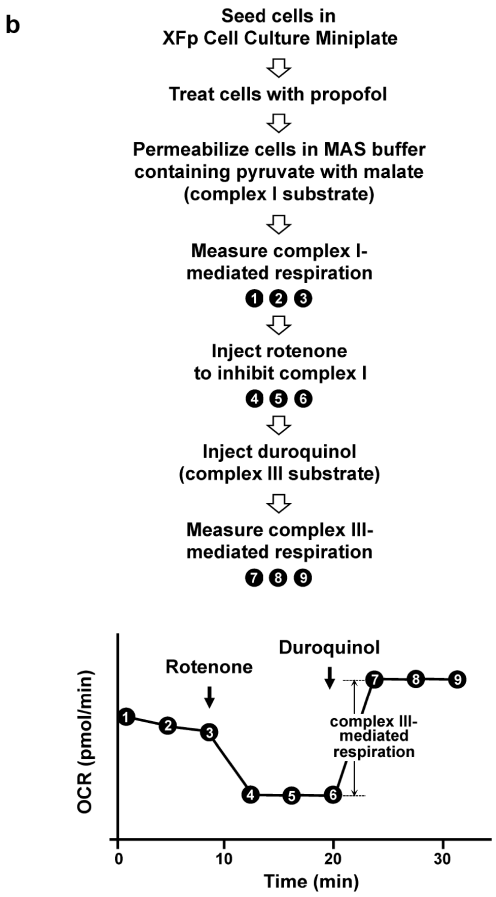

Supplentary Figure 3 | Measurement of oxygen consumption in permeabilized cells

The activity of individual respiratory chain complexes was evaluated by employing specific substrates and inhibitors. (a) Cells were treated with plasma membrane permeabilizer and offered pyruvate and malate for measuring complex I-mediated respiration. Cells were sequentially treated with rotenone (complex I inhibitor), succinate (complex II substrate), antimycin A (complex III inhibitor), and TMPD plus ascorbate (complex IV substrate) as indicated. Oxygen consumption measurements were performed using a Seahorse XFp Extracellular Flux Analyzer. Distinct complex activities were calculated as follows: complex I-mediated respiration = (mean OCR value between points 1 and 2) - (mean OCR value between points 3 and 4); complex II-mediated respiration = (mean OCR value between points 5 and 6) - (mean OCR value between points 3 and 4); complex IV-mediated respiration = (mean OCR value between points 9 and 10) - (mean OCR value between points 7 and 8). (b) Cells were permeabilized as in (a), and treated with rotenone, followed by duroquinol to donate electrons at complex III. Complex III-mediated respiratory activity was calculated as (mean OCR value between points 7-9) - (mean OCR value between points 4-6).

Supplementary Figure 4

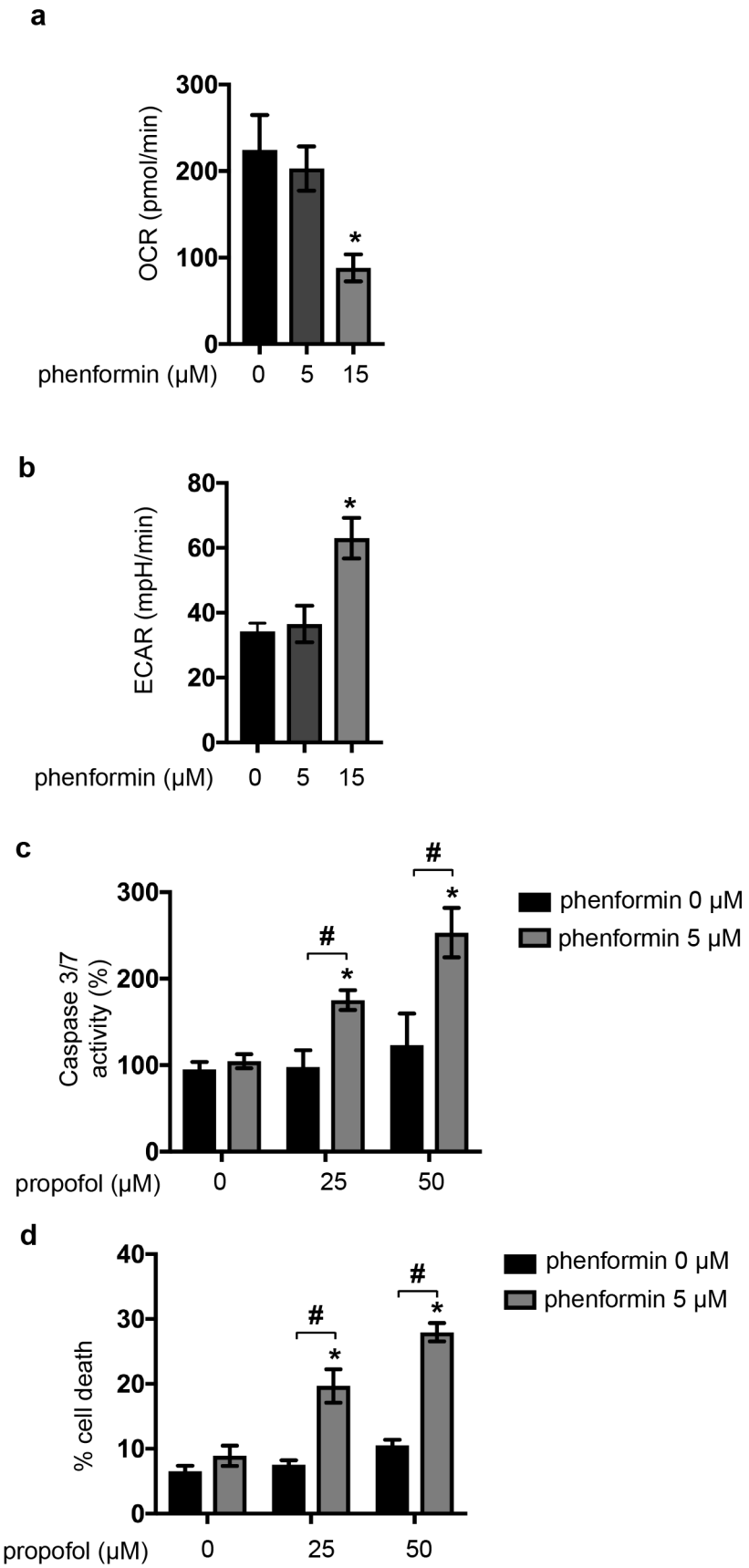

Supplementary Figure 4 | Synergistic effect of propofol with the biguanide phenformin on caspase activity and cell death

Oxygen consumption rate (OCR) (a) and extracellular acidification rate (ECAR) (b) of SH-SY5Y cells exposed to the indicated doses of phenformin (5 and 15 μM) for 6h. SH-SY5Y cells were exposed to the indicated concentrations (25 and 50 μM) of propofol with or without treatment with 5 μM phenformin for 6 h. (c) Graphic depictions of caspase-3/7 (n = 3) activity in each treatment group. (n=3) (d) Cells were harvested and cell death percentages were measured with flow cytometry. The ratio of propidium iodide (PI)-positive and/or annexin V-positive cells [(Q1 + Q2 + Q4)/(Q1 + Q2 + Q3 + Q4)] was used to calculate the percentage of dead cells (n = 3). Data presented in (a)-(d) are expressed as means ± standard deviations (SD). Differences between results were evaluated by the one-way ANOVA followed by Dunnett's multiple comparisons test (a and b) , and two-way ANOVA followed by Dunnett's multiple comparisons test (c and d). *$p < 0.05$ compared to the control cell population.